# Controls on spatial and temporal variability of soil moisture across a heterogeneous boreal forest landscape

Francesco Zignol<sup>1,2</sup>, William Lidberg<sup>1</sup>, Caroline Greiser<sup>1,2,3</sup>, Johannes Larson<sup>1</sup>, Raúl Hoffrén<sup>4</sup>, and Anneli M. Ågren<sup>1</sup>

<sup>5</sup> Department of Forest Ecology and Management, Swedish University of Agricultural Sciences, Umeå, 90183, Sweden

Correspondence to: Francesco Zignol (francesco.zignol@slu.se)

**Abstract.** In light of climate change and biodiversity loss, modeling and mapping soil moisture at high spatiotemporal resolution is increasingly crucial for a wide range of applications in Earth and environmental sciences, particularly in boreal forests, which play a key role in global carbon cycling, are highly sensitive to hydrological changes, and are experiencing rapid warming and more frequent disturbances. However, modeling and mapping soil moisture dynamics is challenging due to the non-linear interactions among numerous physical and biological factors and the wide range of spatial and temporal scales at play. This study aims to identify key spatial and temporal controls on soil moisture using an empirically based modeling approach. We focused on a boreal forest landscape in northern Sweden, where we monitored surface soil moisture with dataloggers at 78 locations during the summer of 2022. We investigated the relationships between observed soil moisture variations and numerous environmental and meteorological predictors from multiple sources at varying spatial resolutions and temporal scales, and we assessed how these relationships changed over time. Spatial variation in soil moisture was influenced not only by topography and by the spatial resolution used to represent it, but also by soil properties, vegetation, and land use/land cover (LULC). In addition, the relative importance of these factors changed over time, with topography generally explaining more spatial variation during wet periods, while soil and vegetation were more relevant during dry periods. This suggests that current soil moisture maps relying primarily on topographic indices could benefit from integrating soil, vegetation, and LULC information to better capture spatial variability under different wetness conditions, as well as from selecting the optimal spatial resolution for the specific area of interest. Temporal variation in soil moisture was better explained by hydrological and meteorological variables averaged over five to seven days preceding soil moisture measurements, highlighting the importance of accounting for both lagged and cumulative effects of weather conditions. Field predictors generally outperformed remote sensing and modeled predictors, indicating that soil moisture mapping based solely on spatially continuous predictors requires improving spatial detail of maps describing soil texture, structure, and organic matter content. Our findings contribute to improving the accuracy and interpretability of data-driven methods, such as machine learning, for mapping soil moisture across space and time for forest management and nature conservation.

<sup>&</sup>lt;sup>2</sup>Bolin Centre for Climate Research, Stockholm University, Stockholm, 10691, Sweden

<sup>&</sup>lt;sup>3</sup>Department of Physical Geography, Stockholm University, Stockholm, 10691, Sweden

<sup>&</sup>lt;sup>4</sup>Department of Geography and Land Management, University of Zaragoza, Zaragoza, 50009, Spain

#### 1 Introduction

45

Soil moisture, often referred to as the water content within the soil, is a key component in modulating terrestrial ecosystem dynamics, playing a crucial role in the water, energy, and biogeochemical cycles at the interface between the atmosphere and the land surface (Seneviratne et al., 2010; Ochsner et al., 2013). In boreal forests, soil moisture has been proven to affect tree growth (Sikström and Hökkä, 2016; Van Sundert et al., 2018; Larson et al., 2024), influence soil nitrogen availability and, in turn, needle production (Nogovitevn et al., 2023), and control the distribution of soil organic carbon stocks (Larson et al., 2023). Modeling the soil moisture state, along with its spatial and temporal fluctuations, is essential for numerous Earth and environmental sciences applications, such as weather forecasting (Collow et al., 2014), water resource management (Dobriyal et al., 2012), forest fire prediction (Chaparro et al., 2016), forest soil trafficability (Schönauer et al., 2024), sustaining ecosystem services (Vereecken et al., 2016), and monitoring ecosystem response to climate change (Jones et al., 2017). Spatial heterogeneity in soil moisture is a key factor in providing diverse habitats, thereby promoting biodiversity (McLaughlin et al., 2017). Temporal variations in soil moisture also influence ecosystem composition, with different species communities depending on more stable or variable soil moisture conditions (Kemppinen et al., 2019). Modeling both components of soil moisture variability assumes even greater significance in the context of climate change and biodiversity loss. In order to accurately model soil moisture, however, it is first necessary to gain a comprehensive understanding of the controls on both spatial patterns and temporal dynamics of soil moisture. Despite the considerable research in this field, most studies primarily focused on the spatial variability of soil moisture, often neglecting temporal variations (Kopecký et al., 2021; Ågren et al., 2021; Zhao et al., 2021), restricted analysis to specific spatial resolutions or temporal scales, overlooking their effects on soil moisture predictions (de Oliveira et al., 2021; Tyystjärvi et al., 2022; Schönauer et al., 2024), or analyzed a partial subset of soil moisture drivers, while omitting others (Potopová et al., 2016; Ge et al., 2022; Larson et al., 2022). For mapping purposes, it is also important to evaluate how well spatially continuous variables (e.g., gridded datasets) perform as predictors of soil moisture compared to field measurements (Zignol et al., 2023). Identifying key predictors of both spatial and temporal soil moisture variability — particularly those derived from remote sensing and modeled products at multiple spatial resolutions and temporal scales — can inform and strengthen data-driven approaches, such as machine learning, by improving both their predictive accuracy and interpretability when mapping soil moisture across space and time.

Factors influencing soil moisture spatiotemporal variability can be classified into five broad groups: topographical features, soil properties, vegetation characteristics, land use/land cover (LULC), and meteorological forcings (Petropoulos et al., 2013; Rasheed et al., 2022). While spatial variations in soil moisture result from the combined effect of multiple types of drivers, most studies have focused on one or two groups (Gwak and Kim, 2017), with topography being considered the most. Due to the ever-higher spatial resolution of digital elevation models (DEMs), such as those derived from airborne light detection and ranging (LiDAR) measurements, researchers have increasingly relied on terrain indices to explain local influences on soil moisture (Murphy et al., 2011; Lidberg et al., 2020; Ågren et al., 2021; Kopecký et al., 2021). However, only a few studies assessed how the spatial resolution of these indices might affect the prediction of soil moisture (Sørensen

and Seibert, 2007; Ågren et al., 2014; Larson et al., 2022). Non-topographical factors usually explain at least half of the spatial variability in soil moisture (Western et al., 1999; Baldwin et al., 2017), and should be taken into account to increase the predictive power of terrain indices (Larson et al., 2022; Kemppinen et al., 2023). Some of these drivers include soil texture (Krauss et al., 2010), soil depth (Tyystjärvi et al., 2022), organic matter content (Amooh and Bonsu, 2015), hydraulic conductivity (Gwak and Kim, 2017), vegetation density (Gwak and Kim, 2017), vegetation type (Gaur and Mohanty, 2013), snow cover (Potopová et al., 2016), tillage (Jonard et al., 2013), and grazing (Zhao et al., 2011). On the other hand, temporal variations in soil moisture are mostly driven by meteorological variables, such as evapotranspiration and precipitation (McMillan and Srinivasan, 2015; Stark and Fridley, 2023), but the relationship between soil moisture and its controlling factors strongly changes depending on the temporal scale considered (Entin et al., 2000; Parent et al., 2006; Chai et al., 2020). A comprehensive investigation of the role of topography, soil, vegetation, LULC, and meteorological variables as well as the effect of their spatial resolution and temporal scale in explaining soil moisture variations is essential for gaining new insights into the key factors driving soil moisture and the optimal spatial resolutions and temporal scales that should be used to predict it.

Research has demonstrated that the relative importance of controls on soil moisture spatial distribution can also vary with changing soil wetness conditions over time (Famiglietti et al., 1998; Western et al., 2004; Joshi and Mohanty, 2010; Mei et al., 2018; Gao et al., 2020; Wang et al., 2023). At the catchment level, the wet state is dominated by lateral surface and subsurface flows, which are influenced by nonlocal controls, primarily macrotopography. Conversely, the dry state is characterized by vertical water fluxes, such as infiltration and evapotranspiration, which are influenced by local controls, mainly soil properties and vegetation (Grayson et al., 1997; Western et al., 1999; Rosenbaum et al., 2012). In cold-climate regions with seasonal snow cover, the relationship between topography and soil moisture is strong after snowmelt but it weakens towards the end of the snowless season when other processes, such as evaporation and transpiration, primarily control soil moisture patterns (Riihimäki et al., 2021; Kemppinen et al., 2023). Similar results emerged from analyses comparing different seasons (Takagi and Lin, 2012) and years (Gaur and Mohanty, 2013), showing that topography explains more variability in soil moisture spatial patterns during the wetter season/year, while soil characteristics play a more prominent role during the drier season/year. However, recent research reveals a more complex relationship, where the influence of topography on soil moisture does not necessarily diminish under dry conditions or increase in wet ones. Instead, the relative importance of terrain metrics has been found to persist or even increase as catchments became drier (Liang et al., 2017; Kaiser and McGlynn, 2018; Han et al., 2021), or to remain low during the wet season (Dymond et al., 2021). Further research is needed to fully understand how the relationship between soil moisture spatial variability and its controls changes in response to different soil wetness conditions. This information holds practical significance for predicting and mapping soil moisture not only spatially, but also over time (e.g., Schönauer et al., 2024).

In predictive models, spatial and temporal variations in soil moisture are commonly estimated by using one of two types of predictors: either point-scale field measurements or gridded datasets derived from remote sensing and other modeling procedures, such as spatial interpolation and data assimilation (e.g., climate reanalyses). In situ observations are typically more

95

accurate but lack spatial continuity, and field campaigns require great efforts in terms of human and financial resources, especially when many environmental variables need to be measured. Conversely, remote sensing and modeled estimates are spatially continuous and can cover large geographic areas, with most datasets being freely available, but they tend to be less accurate than actual measurements. Due to advancements in spatial and temporal resolutions, alongside enhanced algorithms, remote sensing and modeled products are increasingly being employed to predict spatiotemporal variability in soil moisture, gradually replacing, in most instances, in situ observations. While field measurements have been widely used for validation purposes, only a limited number of studies have explicitly compared these two kinds of datasets regarding their predictive capabilities (e.g., Kašpar et al., 2021; Zignol et al., 2023). Remote sensing and modeled gridded predictors have the potential to be used to develop dynamic soil moisture maps over extensive areas, but their predictive performance should be assessed in relation to analogous variables collected in the field.

In this study, we investigated the climatic and environmental factors that determined spatial patterns and temporal dynamics of surface soil moisture measured using 78 dataloggers during three snow-free months in 2022 across a heterogeneous boreal forest landscape in northern Sweden. By taking advantage of extensive field measurements available for the well-studied Krycklan catchment (Laudon et al., 2013, 2021), we were able to analyze a broad range of soil moisture predictors and compare their predictive performance with those of analogous variables obtained from remote sensing or modeled datasets. We tested the hypotheses that the spatial resolution of gridded predictors influences the ability to predict spatial variations in soil moisture, and that meteorological conditions preceding the logger recordings are key to predict its temporal variations. Additionally, we examined whether the relative importance of predictors in explaining spatial variability in soil moisture changes in response to different wetness conditions throughout the study season. With the ultimate purpose of providing insights into data-driven modeling of soil moisture across time and space, we identified four specific aims: (i) to assess how different variables at varying spatial resolutions affect the prediction of soil moisture spatial variability, (ii) to evaluate the relative contribution of numerous meteorological variables at multiple temporal scales in predicting soil moisture temporal variability, (iii) to investigate how varying soil wetness conditions over time impact the ability to explain spatial variations in soil moisture, and (iv) to compare the predictive performance of field measurements versus remote sensing and modeled estimates.

#### 2 Material and methods

#### **2.1 Study area**

The Krycklan catchment covers an area of about 68 km² in northern Sweden (Fig. 1), with elevations ranging between 127 and 372 m a. s. l. (Fig. S1b) (Larson et al., 2022). Soils, lying on a poorly weathered gneiss bedrock, consist primarily of unsorted glacial till (51%) at higher altitudes and postglacial sorted sediments of sand and silt (30%) at lower altitudes (Fig. S1a) (Laudon et al., 2013). In the northern part of the catchment, peat has built up in areas with low topographic relief, typically forming oligotrophic minerogenic mires (8.7%) (Figs. S1a and S1d) (Laudon et al., 2021). The landscape is predominantly

forested (87.5%) (Figs. S1c and S1d), with Scots pine (*Pinus sylvestris*) and Norway spruce (*Picea abies*) as the main tree species (63% and 26%, respectively), and an understory of bilberry (*Vaccinium myrtillus*) and cowberry (*Vaccinium vitisidaea*) on moss mats of *Hylocomium splendens* and *Pleurozium schreberi* (Laudon et al., 2013). The remaining coverage includes arable land (2.0%), open land (0.9%), lakes (0.8%), and a small fraction of urban land (0.03%) (Fig. S1d) (Lantmäteriet, 2023). The area is characterized by a cold temperate humid climate, with a mean annual temperature of 2.1°C and a total annual precipitation of 619 mm, of which over 30% falls as snow (Larson et al., 2022). Approximately 25% of the forested area has been protected since 1922, while the remaining majority consists of second-growth managed forest. Forestry practices have shifted over time, from selective cutting prior to the 1940s to predominantly rotation forestry characterized by clear-cutting and subsequent conifer planting, resulting in a heterogeneous landscape with varying stand ages and species compositions (Laudon et al., 2021).

Since the 1980s, the Krycklan catchment has supported research on ecosystem dynamics and forest management with high-quality, long-term climatic, biogeochemical, hydrological, and environmental measurements, making it a unique field infrastructure in boreal forest landscapes (Laudon et al., 2013). It features 11 gauged streams, around 1000 soil lysimeters, 150 groundwater wells, over 500 permanent forest inventory plots, 3 automatic weather stations (Fig. 1), and a 150 m tall ICOS (Integrated Carbon Observation System) tower (Fig. 1) for measuring atmospheric gas concentrations and biosphere–atmosphere exchanges of carbon, water, and energy (Laudon et al., 2021). Additionally, high-resolution multi-spectral LiDAR measurements and large-scale experiments have been conducted in the Krycklan catchment over the past decade.

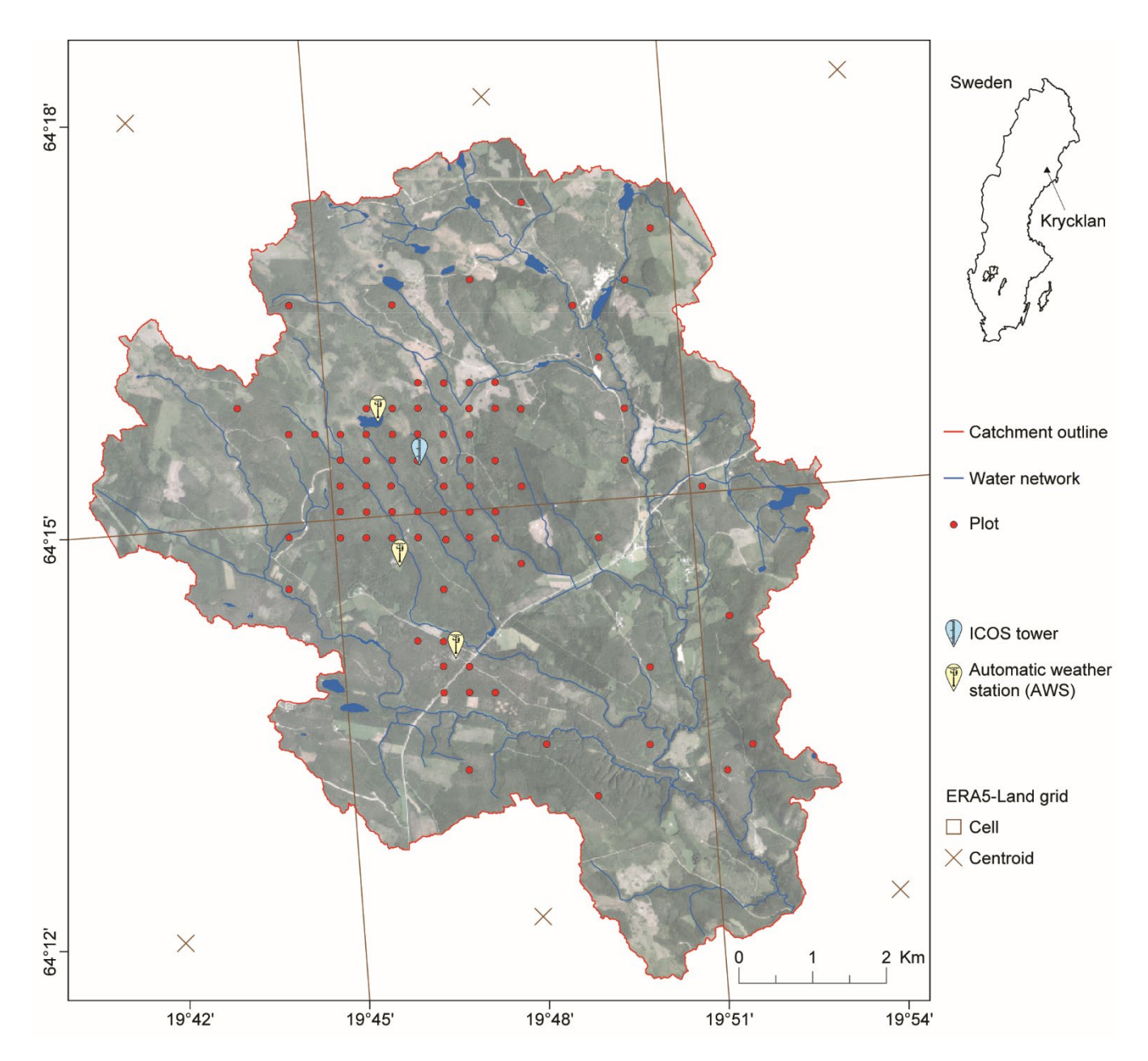


**Figure 1.** Overview of the Krycklan catchment showing the locations of the 78 soil moisture monitoring plots, the three automatic weather stations, and the ICOS tower, with the ERA5-Land grid superimposed. Orthophoto and water network: Lantmäteriet (2021).

#### 2.2 Meteorological and environmental data

150

The extensive field inventory for the Krycklan catchment, combined with remote sensing and modeled data (e.g., from spatial interpolation and data assimilation), enabled us to evaluate a wide range of meteorological and environmental variables as potential predictors of soil moisture, the response variable in our study. We classified predictors into two groups: "spatial"

predictors, which were assumed to be temporally static during the study season but varied spatially, and were used to explain the spatial variability in soil moisture (Table 1); and "temporal" predictors, which varied temporally but not spatially across the study area, and were used to explain the temporal variability in soil moisture (Table 2).

#### 2.2.1 Response variable: soil moisture

160

165

170

175

180

185

To measure soil moisture, we selected a subset of 78 plots (Fig. 1) from a forest survey grid established in 2014 (Larson et al., 2023). This grid consists of 500 equally spaced plots (350 m apart), each of 10 m radius, covering the entire Krycklan catchment. Plot selection was informed by previous research (Larson et al., 2022), which classified most of the 500 plots into five soil moisture classes based on the Swedish National Forest Inventory (NFI) protocol. Our aim was to capture the full range and distribution of soil moisture conditions — from dry ridges to wet peatlands — observed across the Swedish forest landscape (see Fig. 3 in Ågren et al., 2021). To achieve this, approximately half of the selected plots were located in the central part of the catchment (Fig. 1), characterized by a highly heterogeneous landscape with diverse soil moisture conditions (Fig. S1). The remaining loggers were distributed throughout the catchment to ensure adequate spatial coverage while maintaining accessibility.

At each site, we measured soil moisture content of the upper 14 cm of soil at a 15 min resolution using a TOMST TMS logger (Wild et al., 2019). We installed the loggers in June/July 2022 and we downloaded the data in October 2022, covering 92 days for all sites (from July 5 to October 4). Because the sensor in the TMS logger relies on the time domain transmission method (Wild et al., 2019), we converted the raw signals into volumetric water content using the universal calibration equation presented in Kopecký et al. (2021). We also evaluated the soil-specific conversion functions proposed by Wild et al. (2019), but we found that some of the resulting volumetric water content values were nonsensical (e.g., <0% and >100%), particularly in mires. Consistent with findings from other studies in similar landscapes (e.g., Kemppinen et al., 2023), we concluded that these conversion functions were unsuitable for the soil types in Krycklan, specifically peat soils. Because the conversion did not alter the relative order among sites, we eventually adopted the universal curve for all plots, which produced a more realistic range of volumetric water content values.

We plotted each individual time series and conducted a thorough visual inspection to identify any anomalies. We checked for sudden drops in soil moisture that quickly reversed, as these often indicate potential loss of contact between sensor and soil. We carefully removed potentially erroneous data to ensure the reliability of our dataset. From the 15 min time series of volumetric water content, we calculated the mean daily time series for each plot, which served as the response variables in study aim (iii) (Table 3). We then aggregated these data to generate two additional datasets: the seasonal average of mean daily values for each plot and the spatially averaged mean daily time series across all sites, used as the response variables in study aims (i) and (ii), respectively (Table 3). For simplicity, when referring to our analysis, we use the term "soil moisture" in lieu of "volumetric water content at a depth of 0–14 cm".

#### 2.2.2 Spatial predictors: soil, topography, vegetation, and land use/land cover

In addition to monitoring soil moisture, we collected a vast array of environmental variables for each of the 78 plots (Fig. 1 and Table 1). Field variables were selected from the Krycklan inventory or during our field campaigns, whereas non-field variables were extracted from existing vector and raster maps, LiDAR-derived topographic indices, and other remote sensing products. In the case of topographic indices and the normalized difference vegetation index (NDVI), we extracted plot values from layers at different spatial resolutions (0.5, 1, 2, 4, 8, 16, 32, and 64 m for the topographic indices and 0.4, 2, and 30 m for NDVI) to assess how varying spatial resolutions explained soil moisture spatial variability. We also tested the effect of different user-defined thresholds, specifically two vertical distances (2 and 4 m) for the downslope index and six stream initiation thresholds (1, 2, 4, 8, 16, and 32 ha) for depth to water and elevation above stream. To facilitate the visualization and interpretation of the results, all predictors were subdivided into four groups, namely soil, topography, vegetation, and land use/land cover (LULC), and 18 color-coded categories (Table 1). Categories encompass analogous variables from distinct sources (e.g., land cover), diverse measures of a common feature (e.g., forest structure), the same variable at different spatial resolutions and/or user-defined thresholds (e.g., depth to water), or a combination of these cases. Note that classes of qualitative variables were treated as independent predictors in this analysis (e.g., soil survey). Table 1 lists all the spatial predictors evaluated in this study. A detailed description of each can be found in the Supplement.

**Table 1.** All predictors of soil moisture spatial variability evaluated in this study. The 48 predictors are subdivided into four groups and 18 color-coded categories, listed in alphabetical order within each group and category based on the abbreviation code ("Abbr." column). The table also displays the data source (field, non-field raster (N-field r), non-field vector (N-field v)), data type (qualitative (Ql) vs. quantitative (Qn)), and references. Each class of the qualitative variables is considered as a distinct predictor in the analysis. The number of layers of the topographic and vegetation indices is reported in parenthesis after the predictor name, and it depends on: <sup>1</sup> the spatial resolutions (0.5, 1, 2, 4, 8, 16, 32, and 64 m for the topographic indices and 0.4, 2, and 30 m for NDVI); <sup>2</sup> the stream initiation thresholds (1, 2, 4, 8, 16, and 32 ha for depth to water and elevation above stream); and <sup>3</sup> the vertical distances (2 and 4 m for the downslope index). An asterisk denotes the 22 most relevant soil moisture predictors, which are displayed in Fig. 3. The 26 remaining predictors (without asterisk) are shown in Fig. S2. The Supplement provides a detailed description of each variable listed in this table.

Group	Category	Name (number of lay	ers)	Abbr.	Source	Type	Reference
Soil	■ Organic soil	Organic layer thickne	olt	Field	Qn	Zignol et al. (2025)	
	Soil depth	SGU soil depth map		sd-sgu	N-field r	Qn	SGU (2024a)
	Soil moisture	Soil moisture survey	Soil moisture survey *		Field	Qn	Zignol et al. (2025)
	■ Soil type		loamy sand *	ss-losa		Ql	_
		Soil survey	peat *	ss-pt	Field		
			sand	ss-sa			Zignol et al. (2025)
			sandy loam	ss-salo			
			silt loam	ss-silo			
			clay to silt	st-cs		OI.	SGU (2024b)
		SGU Quaternary deposit map	glacifluvial sediment	st-gfs	N-field v Q		
			postglacial sand	st-ps			
			postglacial sand to gravel	st-psg		Qı	300 (20240)
			peat *	st-pt			
			till	st-till			

Group	Category	Name (number of layers)	Abbr.	Source	Type	Reference	
	Depth to water	Depth to water (48) *	dtw <sup>2</sup> -1			Lidberg et al. (2020)	
	Diffuse solar radiation	Diffuse solar radiation (8)	dfr-1			Zignal at al. (2025)	
	Direct solar radiation	Direct solar radiation (8) *	drr-1			Zignol et al. (2025)	
	■ Downslope index	Downslope index (16) *	di <sup>3</sup> -1				
	Elevation above stream	Elevation above stream (48) *	eas2-1	N-field r	Qn		
Topography	■ Landscape wetness Index	Landscape wetness index (8) *	wilt-1			Lidberg et al. (2020)	
	Plan curvature	Plan curvature (8) *	plc-1				
	Relative topographic position	Relative topographic position (8) *	rtp-1				
	■ Topographic wetness index	Topographic wetness index (8) *	twi-1	_1			
		SLU soil moisture map *	sm-slu	N. C. 11		SLU (2021)	
	■ Topography-based map	Soil moisture index map *	smi	N-field r	Qn	Naturvårdsverket (2022)	
		Biomass above ground	bio	Field	Qn	Zignol et al. (2025)	
	■ Forest productivity	SLU forest biomass map	bio-slu		Qn	SLU (2010)	
		Normalized difference vegetation index (3) *	ndvi-1	N-field r	Qn	Lantmäteriet (2021), USGS (2022)	
		Site index by site factors *	sis	Field	Qn	Zignol et al. (2025)	
		Stem density  Volume of birch species	stm bir	Field		Zignol et al. (2025)	
		<u>.</u>	bir-slu	N-field r		. ,	
	■ Species composition	SLU birch map Volume of pine species *		Field		SLU (2010)	
Vegetation		SLU pine map	pi mi alu	N-field r	Qn	Zignol et al. (2025) SLU (2010)	
regetation		1 1	pi-slu	Field			
		Volume of spruce species	spr	N-field r		Zignol et al. (2025)	
		SLU spruce map	1			SLU (2010)	
		Canopy openness	co	F: 11		7: 1 + 1 (2025)	
	■ Forest structure	Basal area weighted mean diameter	dgv	Field		Zignol et al. (2025)	
		Basal area weighted mean height	hgv	hgv-slu N-field r vol Field		GLIL (2010)	
		SLU basal area weighted mean height map	C			SLU (2010)	
		Volume of all tree species				Zignol et al. (2025)	
		SLU forest volume map	vol-slu	N-field r		SLU (2010)	
	■ Land use/land cover	Land map – clearcut		lm-cut		Skogsstyrelsen (2024)	
		Land map – forest *	lm-for	N-field v	QΙ	Lantmäteriet (2023)	
LULC		Land map – peatland *	lm-ptl				
		Land survey – clearcut	ls-cut				
		Land survey – forest *	ls-for	Field	ield Ql Zignol et al.		
		Land survey – peatland *	ls-ptl				

## 210 2.2.3 Temporal predictors: meteorological forcings

For the temporal analysis, we selected meteorological variables (Table 2) from three datasets, including reanalysis data from the land component of the European Centre for Medium-Range Weather Forecasts (ECMWF) Atmospheric Reanalysis Fifth Generation (ERA5-Land) (Muñoz-Sabater, 2019; Muñoz-Sabater et al., 2021), atmospheric data from the ICOS tower (Peichl

et al., 2024), and three automatic weather stations (Svartberget Research Station, 2022a, b, c). For each variable, we generated a single daily time series from July 5 to October 4, 2022, for the entire catchment by calculating the spatial average between either the three weather stations or the six ERA5-Land cells covering the Krycklan area (Fig. 1). To evaluate how varying temporal scales explained temporal variability of soil moisture, we created seven additional time series for each variable based on different temporal scales, including the preceding day and the average between 3, 5, 7, 10, 14, and 21 preceding days. All predictors were subdivided into 12 color-coded categories to facilitate the visualization of the results. These categories group together analogous variables from distinct sources (e.g., precipitation), any variable measured at different depths (e.g., soil water) or heights (air temperature), diverse aspects of the same process (e.g., evaporation), or a combination of these cases. Table 1 lists all the temporal predictors analyzed in this study, with a detailed description of each provided in the Supplement.

**Table 2.** All predictors of soil moisture temporal variability assessed in this study. The 60 predictors are subdivided into 12 color-coded categories, listed in alphabetical order within each category based on the abbreviation code ("Abbr." column). The table also indicates the unit of measurement, the dataset (ERA5-Land, ICOS tower, or weather stations), and data source (field vs. non-field (N-field)). Whenever possible, either the sensor height (field data) or the height of the estimated values (ERA5-Land) is reported in parenthesis after the predictor name. An asterisk denotes the 25 most relevant predictors, which are displayed in Fig. 4. The 35 remaining predictors (without asterisk) are shown in Fig. S3. The Supplement provides a detailed description of each variable listed in this table.

Category	Name (height of sensor or estimated values)	Abbr.	Unit	Dataset	Source
	2 m dewpoint temperature (2 m)	d2m			
	Skin temperature (0 m)	skt		ERA5-Land	N-field
	2 m temperature (2 m)	t2m			
<b>A</b> :	Air temperature (1.7 m)	ta	°C	Weather stations	
Air temperature	Air temperature level 1 (42 m)	ta1	C		
	Air temperature level 2 (30 m) ta2			ICOS tower	Field
	Air temperature level 3 (20 m)	ta3		ICOS tower	
	Air temperature level 4 (10 m)	ta4			
• • •	Air relative humidity (32.5 m) *	rh	%	ICOS tower	Field
Air water	Skin reservoir content *	src	mm	ERA5-Land	N-field
	Total evaporation	e			
	Evaporation from bare soil	ebs			
Evaporation	Potential evaporation *	ep mm, accumulated		ERA5-Land	N-field
	Evaporation from the top of canopy *	etc			
	Evaporation from vegetation transpiration *	evt			
	Soil heat flux level 1 (0 cm)	sh1	W/m²	ICOS tower	Field
■ Heat	Soil heat flux level 2 (5 cm)	sh2	w/m²	icos tower	
	Surface sensible heat flux (0 m) *	shf	J/m², accumulated	ERA5-Land	N-field
<b>- D</b> - 1 1/2 2	Total precipitation *	p	1 . 1	ERA5-Land	N-field
Precipitation	Total precipitation (1.5 m) *	pr	mm, accumulated	Weather stations	Field
	Air pressure (1.7 m) *	pa		Weather stations	Field
<b>.</b> D	Surface pressure (0 m) *	sp hPa		ERA5-Land	N-field
Pressure	Vapor pressure (1.7 m)	vp	пра	Weather stations	Field
	Vapor pressure deficit (32.5 m) *	vpd		ICOS tower	

Category	Name (height of sensor or estimated values)	Abbr.	Unit	Dataset	Source
	Forecast albedo	fal	dimensionless, 0-1	ERA5-Land	N-field
	Long wave incoming radiation (50 m) *	lwi	W//2	ICOS tower	Field
	Long wave outgoing radiation (50 m)	lwo	W/m²	icos tower	ricia
D = 41=41=	Surface net solar radiation (0 m)	nsr	I/m² a a a y may late d	ERA5-Land	N field
Radiation	Surface net thermal radiation (0 m) *	ntr	J/m², accumulated	EKA3-Land	N-field
	Short wave incoming radiation (50 m) *	swi	W//2	ICOS tower	Eigld
	Short wave outgoing radiation (50 m) * swo		W/m²	icos tower	Field
	Surface thermal radiation downwards (0 m) *	trd	J/m², accumulated	ERA5-Land	N-field
	Runoff	ro			
Runoff	Surface runoff (0 m) *	sr	mm, accumulated	ERA5-Land	N-field
	Sub-surface runoff	ssr			
	Soil temperature level 1 (0–7 cm below surface)	st1			N-field
	Soil temperature level 2 (7–28 cm below surface)	st2		EDAGI. 1	
	Soil temperature level 3 (28–100 cm below surface) *	st3		ERA5-Land	
	Soil temperature level 4 (100–289 cm below surface)	st4	0.5		
Soil temperature	Soil temperature level 1 (-10 cm)	ts1	°C	Weather stations	Field
	Soil temperature level 2 (-20 cm)	ts2			
	Soil temperature level 3 (-30 cm) *	ts3			
	Soil temperature level 4 (-50 cm)	ts4		ICOS tower	
	Soil water content level 1 (-2.5 cm) *	sm1		ICOS tower	Field
	Soil water content level 2 (-5 cm)	sm2			
	Soil water content level 3 (-10 cm)	sm3			
	Soil water content level 4 (-30 cm)	sm4			
Soil water	Volumetric soil water level 1 (0-7 cm below surface) *	sw1	%		N-field
	Volumetric soil water level 2 (7–28 cm below surface)	sw2			
	Volumetric soil water level 3 (28–100 cm below surface)	sw3		ERA5-Land	
	Volumetric soil water level 4 (100–289 cm below surface)	sw4			
	Leaf area index, high vegetation	lai	$m^2/m^2$	ERA5-Land	N-field
	Photosynthetic photon flux density below canopy incoming (1.15 m)	pbc		ICOS tower	Field
Vegetation	Photosynthetic photon flux density diffuse (50 m)	pd			
C	Photosynthetic photon flux density incoming (50 m) *	pi	μmolPhotons/m²/s		
	Photosynthetic photon flux density outgoing (50 m) *	po			
	10 m u-component of wind *	u10	,		N-field
= ***	10 m v-component of wind	v10	m/s	ERA5-Land	
Wind	Wind direction respect to geographic north (34.5 m)	wd	degrees N		Field
	Wind speed (34.5 m) *			ICOS tower	

## 2.3 Statistical model

To identify significant predictors of soil moisture, we used orthogonal projections to latent structures (OPLS) analysis, an enhanced version of partial least-squares regression (PLS) (Eriksson et al., 2013). OPLS separates the systematic variation in

the predictors (X) into two parts: a predictive component (horizontal axis) that is directly associated with the response variable of interest (Y) and an orthogonal component (vertical axis) that represents the variation unrelated to Y. This method improves interpretability over ordinary PLS as it allows for identifying key variables for predicting Y while isolating less important variables that contain noise. OPLS is particularly well suited for high-dimensional datasets, as it effectively handles multicollinearity among predictors and reduces the risk of overfitting. In this two-dimensional space, positive or negative loadings on the predictive axis denote variables that are positively or negatively correlated with Y, with stronger correlations as distance from the origin increases. Conversely, loadings on the orthogonal axis, farther from the origin, indicate less correlated variables (i.e., higher noise). In our study, we used soil moisture measurements from dataloggers as the response variable (Y).

We created two types of OPLS models (Table 3). The first type, termed "spatial" OPLS, assessed the role of environmental predictors (soil, topography, vegetation, and LULC) (Table 1) in explaining the observed spatial distribution in soil moisture through direct plot-by-plot comparison. In these models, all environmental predictors varied across Krycklan but were assumed constant over time. Similarly, the response variable was spatially heterogeneous, but only one time step was included in each model. Specifically, to evaluate the relative importance of environmental predictors (aim (i)), we considered the soil moisture seasonal average, whereas to assess how the contribution of these predictors changed over time (aim (iii)), we ran the OPLS model 92 times using soil moisture daily values as the response variable (Table 3). The second type, termed "temporal" OPLS, evaluated the influence of meteorological predictors (Table 2) on the observed daily variations in soil moisture through direct day-by-day comparison (aim (ii)). In this model, all meteorological predictors and the response variable changed daily but were considered uniform across the study area (i.e., we calculated the spatial average) (Table 3).

To evaluate the predictive performance of field versus non-field data (aim (iv)), we ran both the spatial and temporal OPLS models using three different subsets of predictors: (1) only remote sensing and modeled estimates, including gridded and vector datasets such as topographic and vegetation indices and metrics, soil and LULC vector maps, and ERA5-Land time series; (2) only field measurements from surveys or permanent stations (i.e., weather stations and ICOS tower); and (3) a combination of all predictors. To assess the predictive performance of the overall OPLS models, we considered R<sup>2</sup>Y(cum), which represents the cumulative variation in the response variable (i.e., soil moisture) explained by the three subsets of predictors.

To estimate the predictive performance of each variable, we also calculated the variable importance on projection for the predictive component (VIP<sub>predictive</sub>) for the 94 OPLS models based on all predictors (Table 3). These values are normalized such that if each X variable contributed equally to the model, their VIP<sub>predictive</sub> would be 1. Variables with a VIP<sub>predictive</sub> value greater than 1 are considered relevant predictors, with higher scores indicating greater predictive power (Eriksson et al., 2013). We used this metric and threshold to distinguish relevant soil moisture predictors, presented in Figs. 3 and 4, from less important ones, included in the Supplement (Figs. S2 and S3). We processed all the data in R version 4.3.0 (R Core Team, 2023), we generated all OPLS models and calculated the related VIP<sub>predictive</sub> scores in SIMCA 17.0, and we drew all the figures using the R ggplot2 package (Wickham, 2016), ArcGIS Pro (Esri Inc., 2023), and Adobe Illustrator (Adobe Inc., 2024).

**Table 3.** All OPLS models developed in this study.

Aim	Model type	Predictors (X)	Predictors' characteristics	Predictors' subsets	Response variable (Y)	# of models	Figure
(i)	Spatial OPLS	Soil Topography Vegetation LULC	Different spatial resolutions and user-defined thresholds	3 (all, only remote sensing and modeled estimates, only field data)	Seasonal average of mean daily values for each plot	3×1=3	3
(ii)	Temporal OPLS	Meteorological forcings	Different temporal scales	3 (all, only remote sensing and modeled estimates, only field data)	Spatially averaged mean daily time series across all sites	3×1=3	4
(iii)	Spatial OPLS	Soil Topography Vegetation LULC	Different spatial resolutions and user-defined thresholds	3 (all, only remote sensing and modeled estimates, only field data)	Mean daily value of any day within the season for each plot	3×92=276	5

#### 3 Results

270

275

280

#### 3.1 Observed spatial and temporal variability in soil moisture

Analysis of the logger data revealed large spatial variability in both seasonal averages and seasonal standard deviations of soil moisture, ranging from 14% to 56% (~60% = fully saturated) and 0.4% to 5.6%, respectively (Fig. 2a). Among the 78 sites studied, 14 exhibited an increasing trend in soil moisture over the season, seven a decreasing trend, and the remaining 57 no trend, based on the non-parametric Mann-Kendall test (Mann, 1945; Kendall, 1975) at 95% confidence level (Fig. 2bc). The magnitude of soil moisture change over the entire study period, indicated by the trend Theil-Sen's slope (Sen, 1968), varied between -8.4% and 10% (Fig. 2b, Table S1), whereas the strength of the monotonic association between soil moisture and time, as measured by Kendall's correlation coefficient ( $\tau$ ), ranged from -0.58 to +0.57 (Table S1). Daily peaks in soil moisture were typically associated with major precipitation events, although the magnitude of these peaks and subsequent declines during dry periods varied considerably across locations (Fig. 2c). Conversely, the daily spatial variability (i.e., standard deviation) in soil moisture (black line) exhibited a sharp decline during precipitation events (especially in August and September), followed by a steady increase leading up to peaks at the culmination of subsequent dry periods (bottom part of Fig. 2c). The soil moisture time series from ERA5-Land (brown lines) closely tracked the temporal variability of the sites mean (red line), but underestimated daily soil moisture amounts averaged across all sites (Fig. 2c). Overall, Fig. 2 showed that the 78 sites responded differently to similar weather conditions, and that the spatial variability in soil moisture among all sites is much larger than the temporal variability in soil moisture observed throughout the study season.

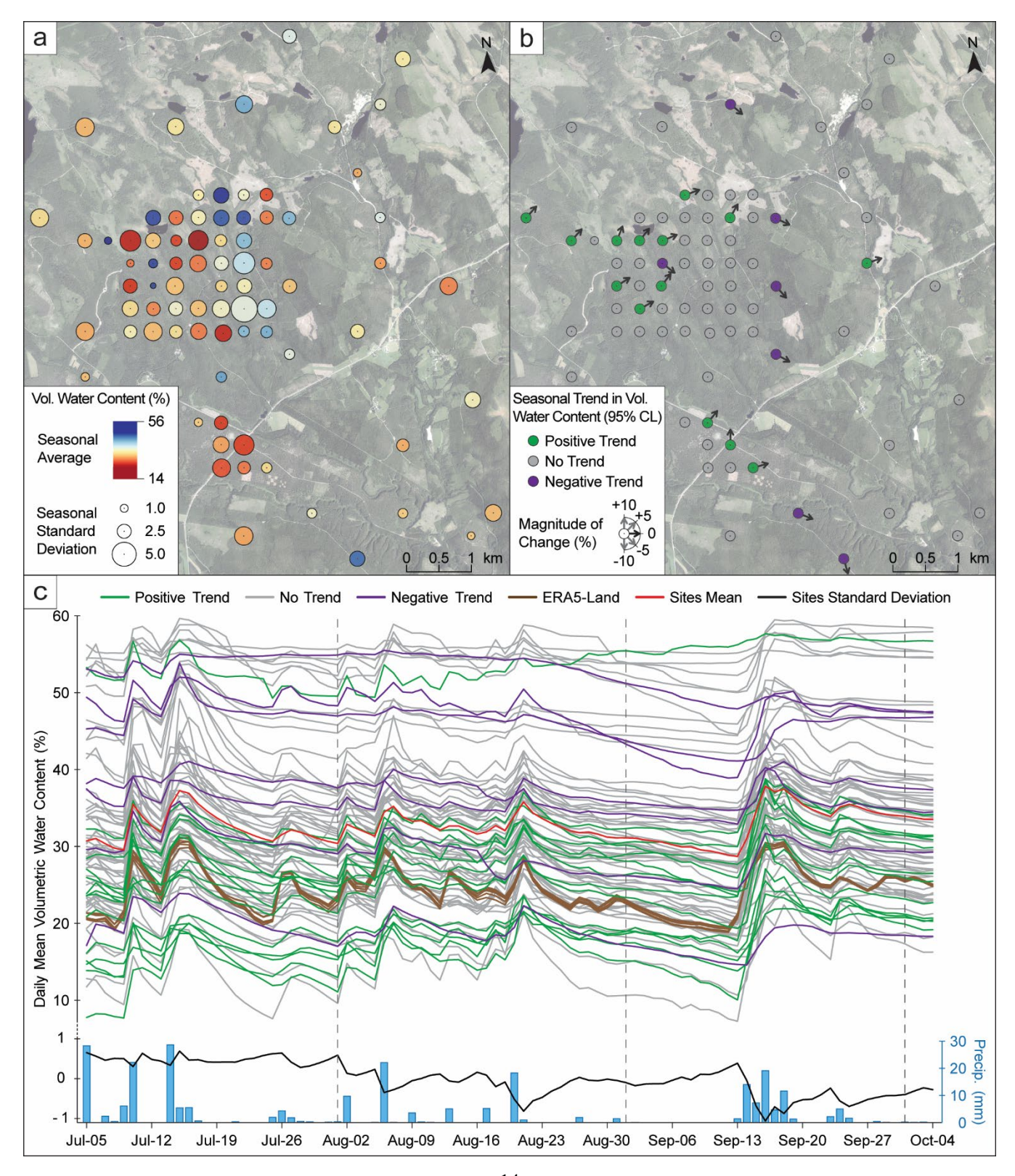


Figure 2. Spatial and temporal variation of daily mean soil moisture (i.e., volumetric water content) measured by 78 loggers across the Krycklan catchment from July 5 to October 4, 2022. (a) Displays the seasonal average and standard deviation of the measurements. (b) Shows seasonal trends identified using the Mann-Kendall test at a 95% confidence interval. (c) Presents the time series plot, with logger data grouped by color according to trend type. The graphic includes additional data for comparison: estimates from six ERA5-Land cells covering the catchment (brown lines), spatial mean (red line) and standard deviation (black line) among sites, and mean precipitation across Krycklan derived from weather stations (bottom bar plot). For clarity, refer to Fig. 1 for the locations of the ERA5-Land cells and weather stations. Orthophoto in panels (a) and (b): Lantmäteriet (2021).

#### 3.2 Controls on soil moisture variability

OPLS plots served as a means to visualize in two dimensions the relative importance of factors controlling soil moisture variability, with loadings located closer to the horizontal axis (i.e., lower noise) and farther from the vertical axis (i.e., higher predictive power) indicating the most relevant predictors. Variables on the right side of the plot are positively correlated to soil moisture, while those on the left side are negatively correlated. Remote sensing and modeled estimates are represented by circles (raster datasets) or rhombuses (vector datasets), whereas field measurements are displayed as triangles. The size of the symbols is proportional to either the spatial resolution or the temporal scale of the potential soil moisture predictors. Variables are grouped together into color-coded categories to facilitate the reading of the OPLS plots. When multiple spatial resolutions or temporal scales were investigated for a certain variable, its loadings were connected through guides transitioning from high to low resolution or scale, and only the optimal resolution or scale was labelled. The upcoming two sections will focus on outlining the key features of the spatial OPLS plot (Figs. 3 and S2) and the temporal OPLS plot (Figs. 4 and S3), respectively. Due to the large amount of variables analyzed in this study, Figs. 3 and 4 only present the most relevant predictors (VIP predictive greater than 1, marked by an asterisk in Tables 1 and 2), whereas all remaining variables are included in the Supplement (Figs. S2 and S3).

#### 3.2.1 Spatial variation

295

300

305

310

315

Relative topographic position emerged as the strongest predictor of soil moisture at a 16 m resolution (rtp-16), but its predictive performance decreased at lower and higher resolutions (Fig. 3). Similar to relative topographic position, depth to water and elevation above stream were negatively correlated with soil moisture, with loadings clustered in the bottom-left quadrant (Figs. 3 and S2). These two indices showed reduced performance and increased noise for higher stream initiation thresholds (Fig. S2). However, while coarse resolution (64 m) was optimal for elevation above stream, high resolution (0.5 or 1 m) was preferable for depth to water (Fig. S2), with eas1-64 and dtw1-05 overall performing best (Fig. 3). In the top-right quadrant (i.e., positively correlated), topographic wetness index and landscape wetness index were good predictors of soil moisture at their optimal resolutions of 32 m (twi-32) and 4 m (wilt-4), respectively (Fig. 3). At these resolutions, they performed comparably to the soil moisture index map (smi) and the SLU soil moisture map (sm-slu), with the last one exhibiting slightly higher performance (Fig. 3). Downslope index and plan curvature at their optimal vertical distance and/or spatial resolution (di2-32 and plc-32), also positively correlated with soil moisture, showed slightly lower predictive power but introduced less

noise (loadings closer to the origin) (Fig. 3). Direct solar radiation was only relevant at a course resolution (drr-64) (Fig. 3), while diffuse solar radiation was a less important predictor (Fig. S2).

320

325

330

As for soil, three field variables — peat soil class (ss-pt), soil moisture classes (sms), and organic layer thickness (olt) — were robust predictors, showing a positive correlation with soil moisture and low noise (Fig. 3). The peat class from the SGU soil type map (st-pt) was also positively correlated, yet it explained less variability than the analogous field predictor (i.e., ss-pt). Both peatland (positively correlated) and forest (negatively correlated) LULC classes similarly revealed that the data collected in the field (ls-ptl and ls-for, respectively) provided slightly better results than using information from an existing map (lm-ptl and lm-for, respectively). Finally, the loamy sand class from the soil survey (ss-losa) was, to a lesser extent, an important predictor, negatively correlated with soil moisture. The remaining soil and LULC variables, whether derived from field observations or existing maps, performed poorly in predicting soil moisture (Fig. S2).

Among the vegetation-related variables, volume of pine (pi) showed the highest predictive performance, followed by the normalized difference vegetation index at 2 m resolution (ndvi-2), and the site index by site factors (sis), with pi and sis being negatively correlated with soil moisture whereas ndvi-2 being positively correlated (Fig. 3). While ndvi-2 and pi slightly outperformed, in terms of predictive power, analogous predictors at courser spatial resolutions (ndvi-30 and pi-slu, respectively), they also introduced more noise (Figs. 3 and S2). The remaining vegetation variables exhibited low predictive performance or high noise, therefore resulting less suitable as soil moisture predictors (Fig. S2).

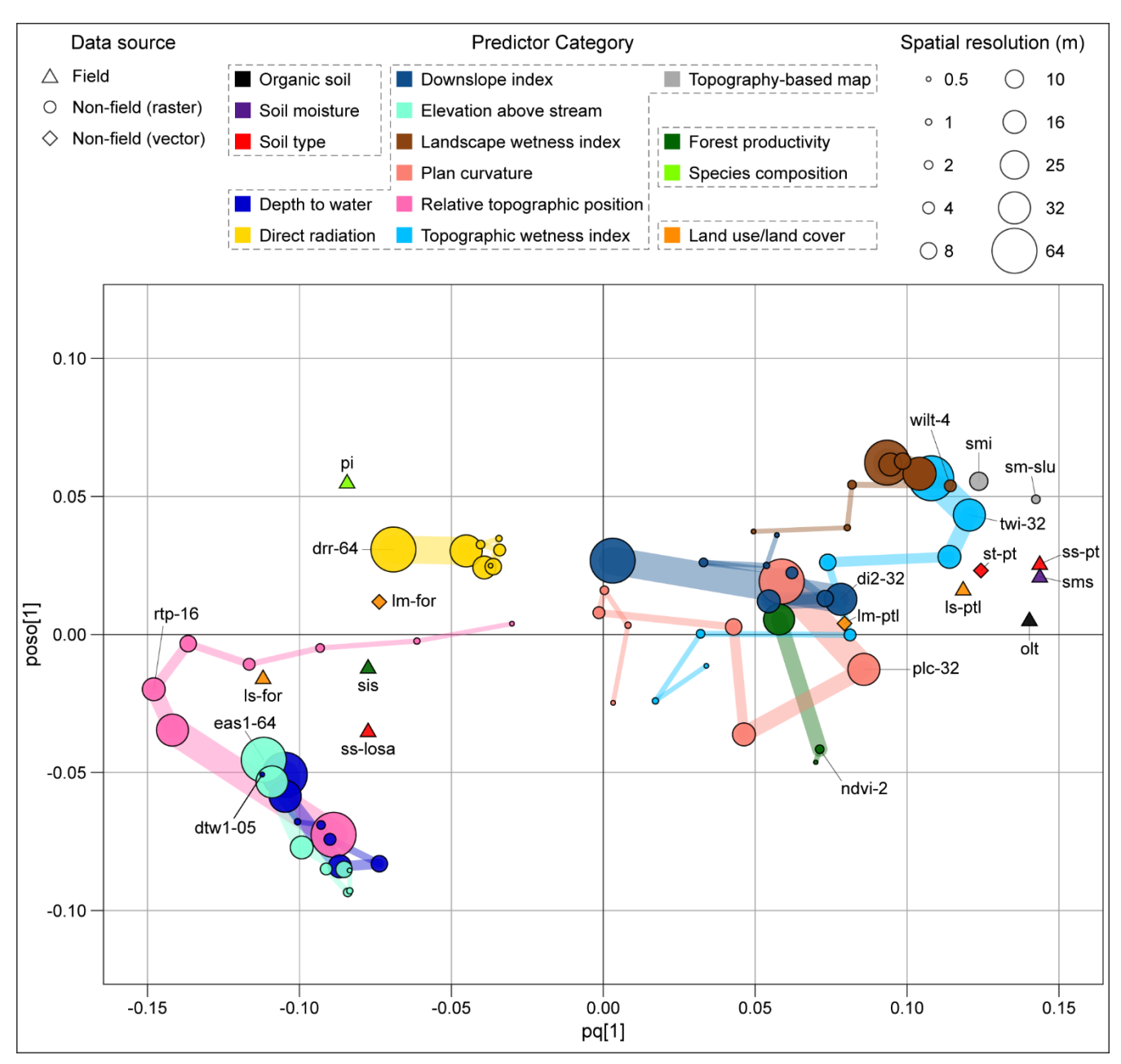


Figure 3. OPLS loading plot showing the relationship between a large array of "spatial" predictors, which vary spatially but remain constant over time, and the mean seasonal soil moisture (July 5 – October 4, 2022). Both the spatial predictors (X-variables) and the determinant (Y-variable) were gathered for 78 sites across the Krycklan catchment (Fig. 1 for the site locations). The spatial predictors, overall describing soil, topography, vegetation, and land use/land cover at each site (grey dotted boxes in the figure legend) were either directly measured in situ (symbolized by triangles) or estimated through remote sensing or modeling techniques (depicted as circles or rhombuses depending on the dataset format). These predictors were organized into 18 color-coded categories (see Table 1; here only 15 are shown) to enhance plot readability. Gridded (i.e., raster) predictors are characterized by a certain spatial resolution (expressed in m, representing the length of the grid cell side), which is proportional to the size of the circles. To visualize the effects of spatial resolution, guides connect loadings of the same variable moving from high to low resolutions, with the variable name visible only in correspondence of the optimal resolution (refer to Table 1 for variable labels). High positive and negative loadings on the predictive axis (pq[1]) represent variables that are positively and

negatively correlated with the response variable (Y), with stronger correlation further away from the origin. The orthogonal axis (poso[1]) indicates how much of the variation for each variable was not correlated with the response variable (Y). This figure only shows the 22 most relevant predictors (VIP<sub>predictive</sub> greater than 1, marked by an asterisk in Table1). If multiple user-defined thresholds were tested for a certain topographic index (i.e., depth to water, downslope index, and elevation above stream), the plot displays only the best-performing one. All 26 remaining variables are included in Fig. S2.

#### 350 3.2.2 Temporal variation

355

360

365

370

Soil moisture estimates from ERA5-Land and ICOS measurements were understandably the two best predictors of the spatially averaged time series of soil moisture recorded at the 78 study plots (Fig. 4). Their predictive performance was highest when selecting the top soil layer and matching the temporal scale with the response variable (sw1-0 and sm1-0). Most loadings of these two predictors were positively correlated with the determinant (Y), though the strength of the correlation generally decreased and noise increased with longer temporal scales and deeper soil layers (Fig. S3).

The temporal OPLS analysis revealed that the optimal temporal scale for most predictors ranged between 5 and 7 days preceding the datalogger recordings, with predictive performance decreasing for both shorter and longer temporal scales (Fig. 4). Skin reservoir content, which accounts for the water in the vegetation canopy and in a thin layer on top of the soil, at the 7-day scale (src-7), emerged as a strong predictor, positively correlated with soil moisture and associated with minimal noise. Surface air pressure at the 7-day scale (sp-7 and pa-7) was also a robust predictor, showing an inverse correlation with soil moisture. Evaporation from the top of canopy at the 5-day scale (etc-5) lay in the vicinity, yet towards higher noise and lower predictive values.

The remaining variables explaining the temporal variability in soil moisture clustered into three distinct areas (Fig. 4). In the right side of the OPLS plot, therefore indicating a positive relationship with soil moisture, two clusters stood out: air relative humidity (rh-7), surface net thermal radiation (ntr-7), surface sensible heat flux (shf-3), evaporation from vegetation transpiration (evt-7), and potential evaporation (ep-5) in the top quadrant; precipitation (pr-7 and p-5), surface runoff (sr-5), long-wave (i.e., thermal) incoming radiation (lwi-5 and trd-5), and wind speed (ws-5) in the bottom quadrant. The third cluster, located in the bottom-left quadrant, consisted of predictors negatively correlated with soil moisture, including incoming and outgoing short wave radiation (swo-5 and swi-5), incoming and outgoing photosynthetic photon flux density (po-5 and pi-5), vapor pressure deficit (vpd-7), 10 m u-component of wind (u10-5), and soil temperature (ts3-21 and st3-21). All air temperature variables, along with other less relevant predictors of soil moisture, are showed in the Supplement (Fig. S3).

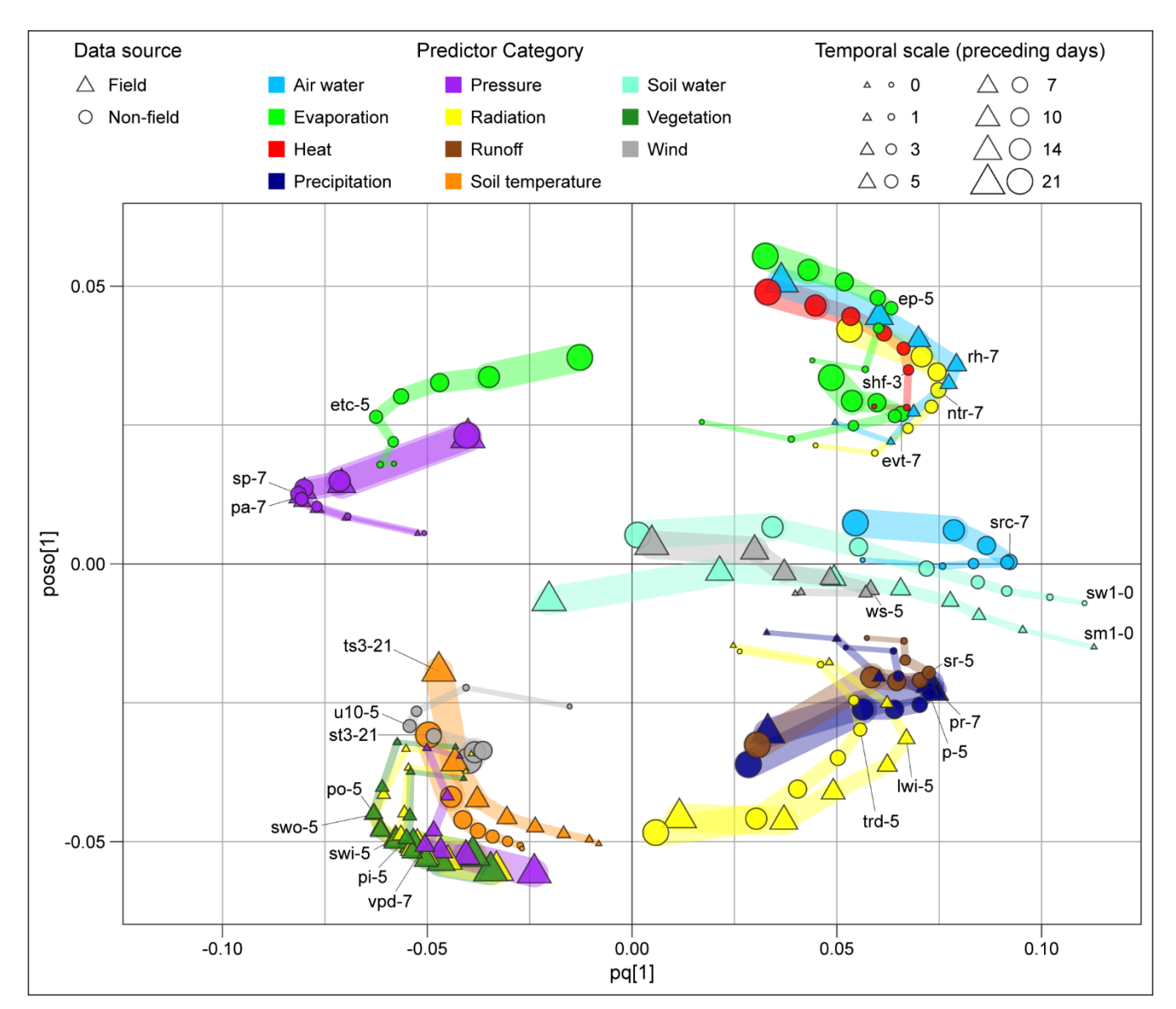


Figure 4. OPLS loading plot illustrating the relationship between a large array of "temporal" predictors, which do not vary spatially but change over time, and daily mean soil moisture (i.e., volumetric water content) averaged across 78 sites within the Krycklan catchment (refer to Fig. 1 for the site locations). Both the temporal predictors (X-variables) and the determinant (Y-variable) were aggregated at the daily temporal scale from July 5 to October 4, 2022. The temporal predictors were either directly measured at the ICOS tower or at weather stations within Krycklan (symbolized by triangles) or extracted from the ERA5-Land dataset (depicted as circles). These predictors were organized into 12 color-coded categories (see Table 2; here only 11 are shown) to enhance plot readability. All predictors are characterized by a certain temporal scale, represented by the size of the triangles or circles. To visualize the effects of temporal scale, guides connect loadings of the same variable moving from high to low scales, with the variable name visible only in correspondence of the optimal scale (refer to Table 2 for variable labels). High positive and negative loadings on the predictive axis (pq[1]) represent variables that are positively and negatively correlated with the response variable (Y), with stronger correlation further away from the origin. The orthogonal axis (poso[1]) indicates how much of the variation for each variable was not correlated with the response variable (Y). This figure only shows the 25 most relevant predictors (VIP<sub>predictive</sub> greater than 1, marked by an asterisk in Table2), but the 35 remaining predictors are included in the Fig. S3.

#### 3.3 Spatial soil moisture variability under different wetness conditions

390

395

400

The relative importance of predictors in influencing spatial soil moisture variability remained relatively consistent over the study period in the Krycklan catchment, with their VIP<sub>predictive</sub> values showing little variation throughout the season (Figs. 5 and S4). The SLU soil moisture map (sm-slu) exhibited the smallest variation among all predictors (seasonal standard deviation of VIP<sub>predictive</sub>: 0.03) (Fig. 5). In contrast, two vegetation-related variables and direct solar radiation (ndvi-2, pi, and ddr-64) showed the largest variation (seasonal standard deviation of VIP<sub>predictive</sub>: 0.09), reflecting generally better performances in the first half of the season (especially at the turn of July and August) compared to the second half (Figs. 5).

Most predictors experienced abrupt drops in VIP<sub>predictive</sub> during intense and/or multi-day precipitation occurrences (e.g., September 16) (Fig. 5), when the soil moisture variability across all 78 sites was also at its lowest (bottom graphic in Fig. 2c). However, some topographic indices (dtw1-05, eas1-64, and, to a lesser degree, plc-32 and rpt-16) showed increasing predictive power after the beginning of a precipitation event (e.g., July 15 or September 15) (Fig. 5). During drying periods (e.g., between late August and almost mid-September), the VIP<sub>predictive</sub> values of the majority of predictors tended to steadily and slowly decrease, except for three notable exceptions: the loamy sand soil class (ss-losa), the site index by site factors (sis), and the downslope index (di2-32).

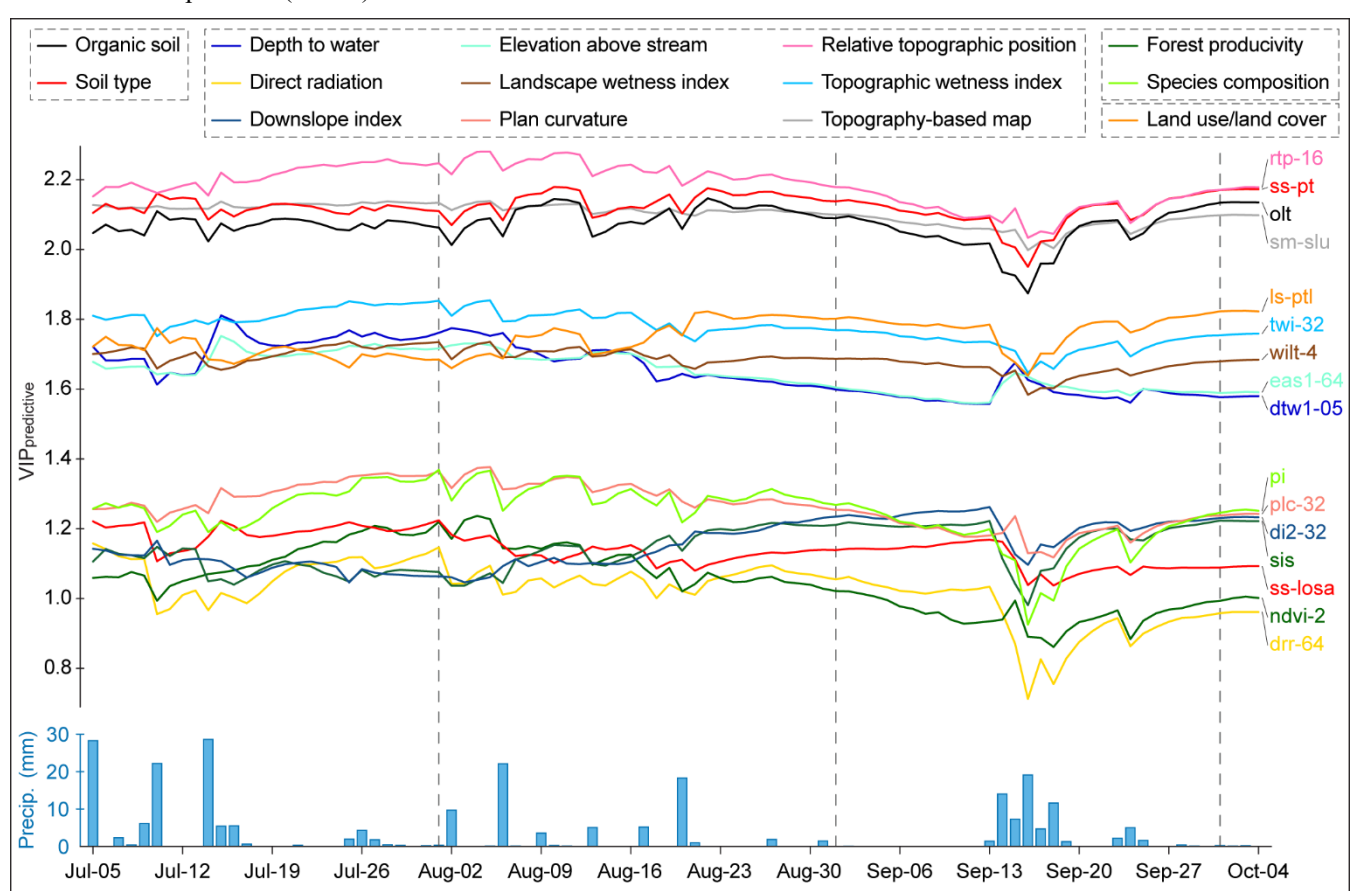


**Figure 5.** VIP<sub>predictive</sub> values of 92 spatial OPLS models generated using mean daily soil moisture over the study season (July 5 – October 4, 2022) as the response variable (Y). The lower section of the figure displays the mean precipitation across Krycklan derived from weather stations (refer to Fig. 1 for their locations). The spatial predictors, overall describing soil, topography, vegetation, and land use/land cover at each site (grey dotted boxes in the figure legend), were organized into 18 color-coded categories (see Table 1; here only 14 are shown) to enhance plot readability. Color-coded labels on the right side of the figure are ordered according to their VIP<sub>predictive</sub> on the last day of the study season (October 4, 2022). To avoid clutter and highlight the key findings, only a subset of predictors is presented, but a graphic with all 22 relevant predictors (VIP<sub>predictive</sub> greater than 1) displayed in Fig. 3 is included in Fig. S4.

#### 3.4 Field measurements compared to remote sensing and modeled estimates

405

410

415

420

Field measurements generally outperformed remote sensing and modeled data by approximately 6% in both spatial and temporal OPLS models, with the combination of all predictors yielding the highest performance (Fig. 6a). In the temporal OPLS models, more variance in soil moisture dynamics was explained by data from the ICOS tower and weather stations ( $R^2Y(cum) = 0.96$ ) compared to ERA5-Land estimates ( $R^2Y(cum) = 0.90$ ). A similar pattern emerged in the spatial OPLS models, where soil, vegetation, and LULC data collected in the field ( $R^2Y(cum) = 0.51$ ) better explained spatial variability in seasonal soil moisture than topographic indices and existing soil, vegetation, and LULC maps ( $R^2Y(cum) = 0.45$ ).

In the spatial OPLS daily models (Fig. 6b), these two subsets of predictors showed the same relative ranking, with field measurements (green line) outperforming remote sensing and modeled estimates (blue line) throughout the season. However, they responded differently to changing wetness conditions. This was most evident between late August and mid-September, a period marked by 24 nearly rain-free days followed by five days of persistent precipitation. R<sup>2</sup>Y(cum) of field-based models (green line) increased sharply during the dry spell, then abruptly dropped by 10% with the onset of rain. In contrast, the models using remote sensing and modeled data showed only a marginal improvement during the dry period and a smaller and more gradual decline (~2%) during rainfall.

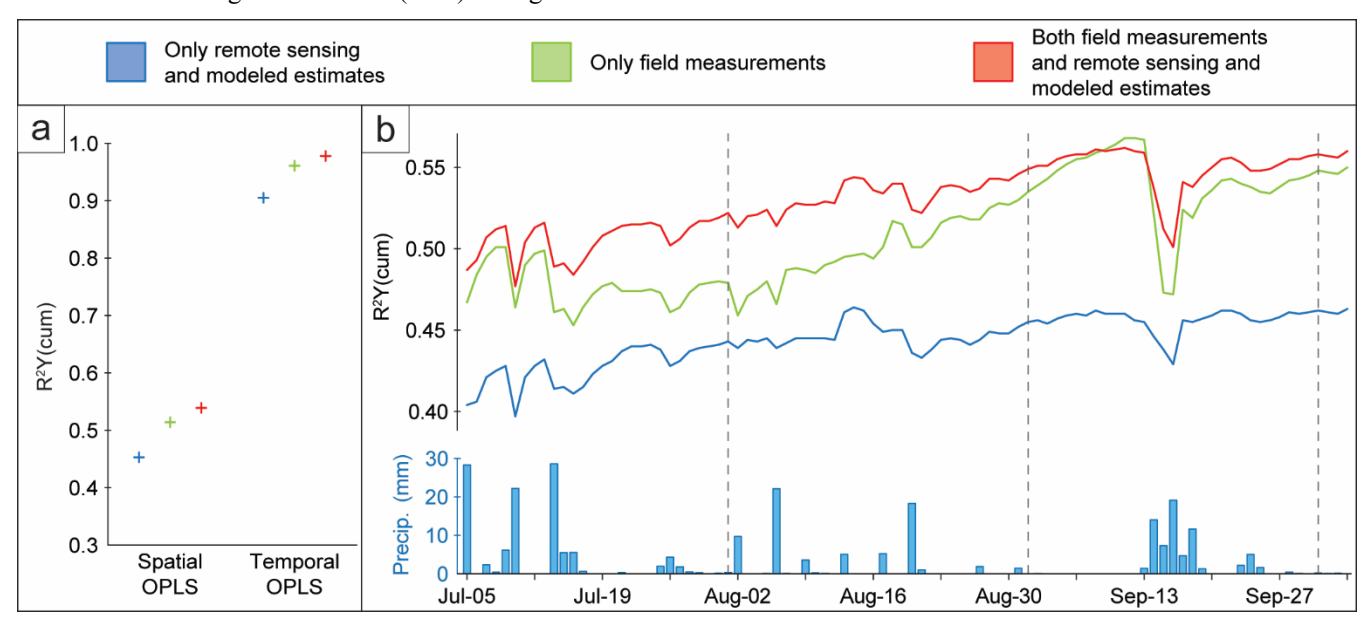


Figure 6. OPLS model performance using only remote sensing and modeled predictors (blue), only field predictors (green), and all predictors combined (red). R<sup>2</sup>Y(cum) indicates the cumulative proportion of variance in the response variable Y (i.e., soil moisture) explained by each

model (see Table 3 for the models' specifications). (a) Shows the R<sup>2</sup>Y(cum) values, indicated by crosses, of models using either the seasonal average per plot (spatial OPLS) or the spatially averaged daily time series across all sites (temporal OPLS) as the response variable. (b) Displays the R<sup>2</sup>Y(cum) values of 92 daily spatial OPLS models over the study period (July 5 – October 4, 2022), with mean precipitation across Krycklan (from weather stations shown in Fig. 1) plotted below for reference.

#### 4 Discussion

In this study, we investigated a vast array of climatic and environmental factors controlling spatial patterns and temporal dynamics of surface soil moisture in a boreal forest landscape in northern Sweden with the purpose of providing new insights into modeling and mapping soil moisture. Specifically, we evaluated the ability of numerous variables extracted from multiple sources, including field measurements, remote sensing retrievals, and modeled data at different spatial resolutions and temporal scales, to explain soil moisture variations recorded during three snow-free months in 2022 by 78 dataloggers distributed across the Krycklan catchment. In the sections that follow, we discuss the primary findings from our analysis.

#### 4.1 Spatial variation

440

445

450

455

We found that all four groups of spatial predictors considered in this analysis, namely topographical features, soil properties, vegetation characteristics, and land use/land cover (LULC), played a significant role in explaining spatial variations in soil moisture (Fig. 3). With the advent of LiDAR-derived DEMs at very high spatial resolution, researchers have increasingly used terrain indices, or a combination of them, as a proxy for soil moisture (Kemppinen et al., 2018; e.g., Kopecký et al., 2021; Riihimäki et al., 2021; Winzeler et al., 2022), including the 10 m resolution soil moisture index map (smi) (Naturvårdsverket, 2022) and the 2 m resolution SLU soil moisture map (sm-slu) (Ågren et al., 2021) that we evaluated in our study. While these maps correlated well with soil moisture measured in the field, our analysis revealed that soil predictors, such as organic layer thickness and soil texture, vegetation-related variables, and land cover information distinguishing between mire and forest were also important. The relevance of integrating soil and terrain information to characterize soil moisture patterns in the context of hydrological modeling was highlighted by similar studies at the catchment scale (e.g., Baldwin et al., 2017). Previous research demonstrated that soil properties were determinant in controlling soil moisture spatial variance at the hillslope (Wang et al., 2023) and regional (Wu et al., 2020) scales as well. Consistent with other studies (e.g., Sørensen and Seibert, 2007; Agren et al., 2014; Lidberg et al., 2020; Larson et al., 2022), our analysis also indicated that the performance of any terrain index varied greatly depending on the threshold and resolution considered, with 1 ha stream initiation threshold providing the best results and 0.5 m spatial resolution being the optimal choice only in one case (i.e., depth to water index). Interestingly, relative topographic position at 16 m resolution (rtp-16) emerged as the best predictor of soil moisture spatial variability, capable of identifying wetter depressions and drier ridges in the landscape (Weiss, 2001). While several examples in the literature demonstrate the importance of this index in soil moisture estimation (e.g., Engstrom et al., 2005; Zhao et al., 2021), it is somewhat surprising that Larson et al. (2022), who used five soil moisture classes estimated in the field as the response variable (sms predictor in our study) (see Table 1 and Fig. 3), observed that relative topographic position was not among the best performing variables in the Krycklan catchment. Therefore, in the pursuit of estimating spatial variability in soil moisture, we advise caution when selecting terrain indices and their spatial resolutions and thresholds. We argue that an enhanced spatial resolution in topographical data does not necessarily compensate for the absence of soil, vegetation, and LULC information. We finally reiterate the importance of soil moisture datalogger measurements to validate predictive models.

#### 4.2 Temporal variation

460

465

470

475

480

485

Our research demonstrated that daily soil moisture fluctuations within the Krycklan catchment are strongly influenced by the hydrological and meteorological conditions over five to seven days preceding soil moisture measurements, regardless of whether these conditions were estimated (ERA5-Land dataset) or measured directly in the field (weather stations and ICOS tower) (Fig. 4). Among other variables, increased soil moisture was correlated with lower air pressure, shortwave radiation, vapor pressure deficit, and evaporation from the top of canopy; conversely, it was associated with higher thermal (longwave) radiation, precipitation, air humidity, evapotranspiration, and wind speed. Averaged conditions over five to seven days for all these variables exhibited the strongest correlation with daily variations in soil moisture in Krycklan, indicating both lagged and cumulative effects of these processes on soil moisture. Previous research has also highlighted the importance of considering multi-day accumulations and time lags between meteorological drivers and soil moisture response (Williams et al., 2009; Pan, 2012; Li et al., 2024), with most studies focusing on precipitation—soil moisture relationship. Parent et al. (2006) showed that the transfer of energy from precipitation to soil moisture via infiltration, percolation, and redistribution processes mostly occurs over temporal scales ranging between 2 and 14 days. Piao et al. (2009) proved that precipitation frequency can be a more crucial factor than precipitation amount in shaping soil moisture variations, making it essential to account for the cumulative effect of precipitation over multi-day temporal scales (Ge et al., 2022). Our study identified soil temperature (28– 100 cm below surface) as the most notable exception to the optimal temporal scale of five to seven days observed for almost all other relevant predictors. While we found a negative correlation between soil temperature and soil moisture as expected (Aalto et al., 2013), the strongest effects emerged at the 3-week scale (the longest temporal scale considered in our analysis), possibly because soil temperature at those depths (28–100 cm) also varies more slowly compared to topsoil temperature. Soil temperature, along with air temperature — which showed weak correlation with soil moisture in our study — might better correlate with soil moisture over longer temporal scales, such as seasonal or annual (Liang et al., 2024). In regard to our findings, it is important to acknowledge that the optimal temporal scale for estimating daily fluctuations in soil moisture can vary according to soil drainage conditions (Parent et al., 2006) and initial wetness conditions characterizing specific climate zones (Chai et al., 2020) or resulting from different seasonal and annual variations in large-scale climate patterns (Li et al., 2024).

#### 4.3 Temporal stability of soil moisture patterns

Different initial wetness conditions can also influence the processes controlling spatial variability in soil moisture (Famiglietti et al., 1998; Western et al., 2004; Joshi and Mohanty, 2010; Mei et al., 2018; Gao et al., 2020; Wang et al., 2023). Although the ranking among predictors remained nearly constant over the study season, we observed that their predictive power changed

490 non-uniformly in relation to daily fluctuations in wetness conditions (i.e., variables responded differently to the same wetness conditions in any day) (Fig. 5). Previous studies indicated that, under drying conditions, lateral water movement is gradually replaced by vertical water movement (Grayson et al., 1997; Western et al., 1999; Rosenbaum et al., 2012), and the spatial variability in soil moisture is likely due to diverse infiltration and evapotranspiration rates related to the spatial distribution of soil and vegetation features (Teuling and Troch, 2005; Takagi and Lin, 2012; Jia et al., 2013; Launiainen et al., 2019). 495 Conversely, the soil moisture spatial variability under rewetting conditions is mostly determined by topographical structures that guide lateral subsurface flow and surface runoff (Grayson et al., 1997; Gaur and Mohanty, 2013). These findings are in line with the results of our study, suggesting that higher infiltration rates in loamy sand soils compared to other soil types and diverse evapotranspiration rates associated to different vegetation (i.e., different site index values) increasingly contributed to the observed spatial distribution of soil moisture particularly during drying periods (e.g., late August to mid-September in our 500 case), while most topographic variables became steadily less relevant during this time. On the other hand, during large precipitation events, topographic indices showed an initial drop in the predictive power likely due to the accumulation of water in the top soil layer and the consequent reduced spatial variability in soil moisture among sites, followed by a time-lagged peak in the predictive power, likely associated with the beginning of lateral subsurface flow driven by topographical features (Grabs et al., 2012). Regarding vegetation, we also observed a clear seasonal pattern: during the peak of the growing season, generally 505 characterized by warmer and longer days, the spatial heterogeneity of vegetation usually had a larger effect on soil moisture distribution. This may be due to stronger effects of increased transpiration or shading during this period, leading to more pronounced differences across plots, whereas this influence diminished towards the end of the summer, when days were usually cooler and shorter. Seasonal patterns in solar radiation affected evapotranspiration rates and soil moisture levels differently not only in forests compared to peatlands, with forests responding more strongly due to higher canopy cover and biomass 510 (Mackay et al., 2007), but also depending on tree species composition, with pine being potentially more responsive to high radiation than spruce (Lagergren and Lindroth, 2002). These findings reiterate the importance of considering the temporal stability of spatial soil moisture patterns under changing wetness conditions (Wang et al., 2023), and we suggest that future research should focus on modeling soil moisture dynamics over longer time scales, beyond a single growing season, particularly in high-latitude environments, where this remains an underexplored topic.

#### 4.4 Mapping spatiotemporal variability in soil moisture

515

520

While there exists an extensive literature assessing the accuracy of remote sensing and modeled estimates of soil moisture based on analogous data measured in situ (Romano, 2014; Petropoulos et al., 2015; Dorigo et al., 2021), we are not aware of any study explicitly comparing the ability of numerous field versus non-field environmental and climate predictors in explaining spatial and temporal variations in soil moisture. Field measurements generally outperformed remote sensing and modeled data, both in terms of overall model performance (Fig. 6) and when comparing pairs of analogous variables from different sources, especially in the case of spatial variability (Figs. 4 and S2). However, field data alone, which included soil, vegetation, and LULC information, did not yield the highest performance, as DEM-derived topographic information also

proved essential, with both types of predictors influencing soil moisture differently depending on prevailing weather conditions (Figs. 5 and 6). We also acknowledge that, even when combining both field and non-field environmental variables in our models, the spatial distribution of soil moisture was not fully captured. In part, this may be explained by measurement inaccuracies, including errors in soil moisture datalogger recordings, and temporal discrepancies in data collection, with some data measured or recorded prior to the 2022 study season (see Supplement). Moreover, we assumed spatial homogeneity for meteorological forcings across the Krycklan catchment, a reasonable assumption for variables like precipitation, but less so for variables such as soil and air temperatures (Aalto et al., 2022; Kolstela et al., 2024), whose fine scale variations likely influenced soil moisture patterns. At even finer spatial scales, variations in soil moisture may have stemmed from local factors not represented by our predictors, such as soil discontinuities, small understory vegetation, and the presence of stones (Parajuli et al., 2020). Future studies should focus on analyzing soil moisture datasets with higher temporal variability (e.g., covering the entire snow-free season, including post-snowmelt periods, and multiple seasons or years), evaluating more accurate LiDAR-derived vegetation metrics, accounting for microclimatic variations, and comparing catchments with diverse characteristics (e.g., spanning a large latitudinal gradient). For future soil moisture mapping, greater efforts should be devoted to improving the quality and resolution of spatially continuous soil information. The lack of detailed soil maps describing soil properties such as texture, structure, and organic matter content was most likely the major cause behind the relatively lower predictive performance of remote sensing and modeled data compared to field data. Enhanced soil maps would benefit not only data-driven approaches to soil moisture mapping but also physically based modeling efforts that rely on such inputs. Informed by the results of this study, we are now able to select a smaller subset of key spatial and temporal predictors of soil moisture, which, in the future, could be integrated into a machine learning model to generate dynamic soil moisture maps for Krycklan. While machine learning models can handle high dimensional data, pre-selecting variables enhances interpretability, reduces overfitting, and ensures that inputs reflect the variation most relevant to soil moisture dynamics (Meyer et al., 2019). Due to their ability to process large volumes of data, such models can leverage detailed spatial and temporal information from multiple sources to potentially map soil moisture at both high spatial and temporal resolutions across vast geographic areas.

#### **5** Conclusions

525

530

535

540

545

550

The Krycklan field infrastructure provided a unique setting for designing a comprehensive study to advance our understanding of the relationship between surface soil moisture and its controls in a forest boreal landscape. By combining remote sensing and modeled data with field measurements across 78 sites in the Krycklan catchment, this study is among the first to examine such a broad range of climatic and environmental factors at different spatial resolutions and temporal scales, focusing on both the spatial and temporal components of soil moisture variability. Our findings suggest that topographical features, soil properties, vegetation characteristics, land use/land cover, and meteorological forcings should all be included when modeling and mapping variations in soil moisture. We highlight the importance of identifying the optimal spatial resolution and temporal scale for each predictor and considering the dynamic nature of the relationship between soil moisture and its controls, which

varies over time. Our results support the development of more accurate and interpretable data-driven models for mapping soil moisture in space and time.

#### Data availability

560

565

575

The soil moisture time series from the TOMST loggers, their geographic locations within the Krycklan catchment, the field survey data listed in Table 1, and the topographic solar radiation data are available at https://doi.org/10.17632/s8zg5ymkh6.1 (Zignol et al., 2025)

#### **Author contribution**

FZ, AÅ, and WL were responsible for the conceptualization of the study. FZ, CG, JL, and RH conducted fieldwork. WL and JL provided the data for the terrain indices. FZ was responsible for the data processing and analysis, prepared the manuscript including all figures, and led the writing of the paper with contributions from all the co-authors. Funding acquisition AÅ, WL, and CG.

#### **Competing interests**

The authors declare that they have no conflict of interest.

#### Acknowledgements

We thank the skilled scientists, technicians, and students that have collated the massive amount of data available for the Krycklan catchment.

#### Financial support

This work was funded by The Swedish Research Council Formas (proj no. 2021–00713, 2021–00115 to AÅ, and 2021–01993 to CG) and Knut and Alice Wallenberg Foundation (2018–0259 Future Silviculture). This work was partially supported by the Wallenberg AI, Autonomous Systems and Software Program – Humanities and Society (WASP-HS) funded by the Marianne and Marcus Wallenberg Foundation, the Marcus and Amalia Wallenberg Foundation. The funding sources had no involvement in the study design and collection, analysis and interpretation of data, nor in the writing of the report.

# Supplement

Supplementary materials associated with this article can be found, in the online version, at link.

#### References

- 580 Aalto, J., le Roux, P. C., and Luoto, M.: Vegetation Mediates Soil Temperature and Moisture in Arctic-Alpine Environments, Arctic, Antarctic, and Alpine Research, 45, 429–439, https://doi.org/10.1657/1938-4246-45.4.429. 2013.
- Aalto, J., Tyystjärvi, V., Niittynen, P., Kemppinen, J., Rissanen, T., Gregow, H., and Luoto, M.: Microclimate temperature variations from boreal forests to the tundra, Agricultural and Forest Meteorology, 323, 109037, 585 https://doi.org/10.1016/j.agrformet.2022.109037, 2022.
  - Adobe Inc.: Adobe Illustrator, Version 28.2, 2024.
  - Ågren, A. M., Lidberg, W., Strömgren, M., Ogilvie, J., and Arp, P. A.: Evaluating digital terrain indices for soil wetness mapping – a Swedish case study, Hydrology and Earth System Sciences, 18, 3623–3634, https://doi.org/10.5194/hess-18-3623-2014, 2014.
- 590 Ågren, A. M., Larson, J., Paul, S. S., Laudon, H., and Lidberg, W.: Use of multiple LIDAR-derived digital terrain indices and machine learning for high-resolution national-scale soil moisture mapping of the Swedish forest landscape, Geoderma, 404, 115280, https://doi.org/10.1016/j.geoderma.2021.115280, 2021.
  - Amooh, M. K. and Bonsu, M.: Effects of Soil Texture and Organic Matter on the Evaporative Loss of Soil Moisture, Journal of Global Agriculture and Ecology, 2015.
- Baldwin, D., Naithani, K. J., and Lin, H.: Combined soil-terrain stratification for characterizing catchment-scale soil 595 moisture variation, Geoderma, 285, 260–269, https://doi.org/10.1016/j.geoderma.2016.09.031, 2017.
  - Chai, O., Wang, T., and Di, C.: Evaluating the impacts of environmental factors on soil moisture temporal dynamics at different time scales, Journal of Water and Climate Change, 12, 420–432, https://doi.org/10.2166/wcc.2020.011, 2020.
- Chaparro, D., Vall-llossera, M., Piles, M., Camps, A., Rüdiger, C., and Riera-Tatché, R.: Predicting the Extent of Wildfires 600 Using Remotely Sensed Soil Moisture and Temperature Trends, IEEE Journal of Selected Topics in Applied Earth Observations and Remote Sensing, 9, 2818–2829, https://doi.org/10.1109/JSTARS.2016.2571838, 2016.
  - Collow, T. W., Robock, A., and Wu, W.: Influences of soil moisture and vegetation on convective precipitation forecasts over the United States Great Plains, Journal of Geophysical Research: Atmospheres, 119, 9338–9358, https://doi.org/10.1002/2014JD021454, 2014.
- 605 Dobriyal, P., Qureshi, A., Badola, R., and Hussain, S. A.: A review of the methods available for estimating soil moisture and its implications for water resource management, Journal of Hydrology, 458–459, 110–117, https://doi.org/10.1016/j.jhydrol.2012.06.021, 2012.
- Dorigo, W., Himmelbauer, I., Aberer, D., Schremmer, L., Petrakovic, I., Zappa, L., Preimesberger, W., Xaver, A., Annor, F., Ardö, J., Baldocchi, D., Bitelli, M., Blöschl, G., Bogena, H., Brocca, L., Calvet, J.-C., Camarero, J. J., Capello, G., Choi, M., Cosh, M. C., van de Giesen, N., Hajdu, I., Ikonen, J., Jensen, K. H., Kanniah, K. D., de Kat, I., Kirchengast, 610 G., Kumar Rai, P., Kyrouac, J., Larson, K., Liu, S., Loew, A., Moghaddam, M., Martínez Fernández, J., Mattar Bader, C., Morbidelli, R., Musial, J. P., Osenga, E., Palecki, M. A., Pellarin, T., Petropoulos, G. P., Pfeil, I., Powers, J., Robock, A., Rüdiger, C., Rummel, U., Strobel, M., Su, Z., Sullivan, R., Tagesson, T., Varlagin, A., Vreugdenhil, M., Walker, J., Wen, J., Wenger, F., Wigneron, J. P., Woods, M., Yang, K., Zeng, Y., Zhang, X., Zreda, M., Dietrich, S., 615 Gruber, A., van Oevelen, P., Wagner, W., Scipal, K., Drusch, M., and Sabia, R.: The International Soil Moisture

- Network: serving Earth system science for over a decade, Hydrology and Earth System Sciences, 25, 5749–5804, https://doi.org/10.5194/hess-25-5749-2021, 2021.
- Dymond, S. F., Wagenbrenner, J. W., Keppeler, E. T., and Bladon, K. D.: Dynamic Hillslope Soil Moisture in a Mediterranean Montane Watershed, Water Resources Research, 57, e2020WR029170, https://doi.org/10.1029/2020WR029170, 2021.
  - Engstrom, R., Hope, A., Kwon, H., Stow, D., and Zamolodchikov, D.: Spatial distribution of near surface soil moisture and its relationship to microtopography in the Alaskan Arctic coastal plain, Hydrology Research, 36, 219–234, https://doi.org/10.2166/nh.2005.0016, 2005.
- Entin, J. K., Robock, A., Vinnikov, K. Y., Hollinger, S. E., Liu, S., and Namkhai, A.: Temporal and spatial scales of observed soil moisture variations in the extratropics, Journal of Geophysical Research: Atmospheres, 105, 11865–11877, https://doi.org/10.1029/2000JD900051, 2000.
  - Eriksson, L., Byrne, T., Johansson, E., Trygg, J., and Vikström, C.: Multi- and Megavariate Data Analysis Basic Principles and Applications, Third revised ed., Umetrics Academy, 509 pp., 2013.
  - Esri Inc.: ArcGIS Pro, Version 3.1.1, 2023.
- Famiglietti, J. S., Rudnicki, J. W., and Rodell, M.: Variability in surface moisture content along a hillslope transect:

  Rattlesnake Hill, Texas, Journal of Hydrology, 210, 259–281, https://doi.org/10.1016/S0022-1694(98)00187-5, 1998.
  - Gao, L., Peng, X., and Biswas, A.: Temporal instability of soil moisture at a hillslope scale under subtropical hydroclimatic conditions, CATENA, 187, 104362, https://doi.org/10.1016/j.catena.2019.104362, 2020.
- Gaur, N. and Mohanty, B. P.: Evolution of physical controls for soil moisture in humid and subhumid watersheds, Water Resources Research, 49, 1244–1258, https://doi.org/10.1002/wrcr.20069, 2013.
  - Ge, F., Xu, M., Gong, C., Zhang, Z., Tan, Q., and Pan, X.: Land cover changes the soil moisture response to rainfall on the Loess Plateau, Hydrological Processes, 36, e14714, https://doi.org/10.1002/hyp.14714, 2022.
- Grabs, T., Bishop, K., Laudon, H., Lyon, S. W., and Seibert, J.: Riparian zone hydrology and soil water total organic carbon (TOC): implications for spatial variability and upscaling of lateral riparian TOC exports, Biogeosciences, 9, 3901–3916, https://doi.org/10.5194/bg-9-3901-2012, 2012.
  - Grayson, R. B., Western, A. W., Chiew, F. H. S., and Blöschl, G.: Preferred states in spatial soil moisture patterns: Local and nonlocal controls, Water Resources Research, 33, 2897–2908, https://doi.org/10.1029/97WR02174, 1997.
  - Gwak, Y. and Kim, S.: Factors affecting soil moisture spatial variability for a humid forest hillslope, Hydrological Processes, 31, 431–445, https://doi.org/10.1002/hyp.11039, 2017.
- 645 Han, X., Liu, J., Srivastava, P., Liu, H., Li, X., Shen, X., and Tan, H.: The Dominant Control of Relief on Soil Water Content Distribution During Wet-Dry Transitions in Headwaters, Water Resources Research, 57, e2021WR029587, https://doi.org/10.1029/2021WR029587, 2021.
  - Jia, Y.-H., Shao, M.-A., and Jia, X.-X.: Spatial pattern of soil moisture and its temporal stability within profiles on a loessial slope in northwestern China, Journal of Hydrology, 495, 150–161, https://doi.org/10.1016/j.jhydrol.2013.05.001, 2013.

- Jonard, F., Mahmoudzadeh, M., Roisin, C., Weihermüller, L., André, F., Minet, J., Vereecken, H., and Lambot, S.: Characterization of tillage effects on the spatial variation of soil properties using ground-penetrating radar and electromagnetic induction, Geoderma, 207–208, 310–322, https://doi.org/10.1016/j.geoderma.2013.05.024, 2013.
- Jones, L. A., Kimball, J. S., Reichle, R. H., Madani, N., Glassy, J., Ardizzone, J. V., Colliander, A., Cleverly, J., Desai, A.
   R., Eamus, D., Euskirchen, E. S., Hutley, L., Macfarlane, C., and Scott, R. L.: The SMAP Level 4 Carbon Product for
   Monitoring Ecosystem Land–Atmosphere CO2 Exchange, IEEE Transactions on Geoscience and Remote Sensing, 55,
   6517–6532, https://doi.org/10.1109/TGRS.2017.2729343, 2017.
  - Joshi, C. and Mohanty, B. P.: Physical controls of near-surface soil moisture across varying spatial scales in an agricultural landscape during SMEX02, Water Resources Research, 46, https://doi.org/10.1029/2010WR009152, 2010.
- Kaiser, K. E. and McGlynn, B. L.: Nested Scales of Spatial and Temporal Variability of Soil Water Content Across a

  Semiarid Montane Catchment, Water Resources Research, 54, 7960–7980, https://doi.org/10.1029/2018WR022591,
  2018.
  - Kašpar, V., Hederová, L., Macek, M., Müllerová, J., Prošek, J., Surový, P., Wild, J., and Kopecký, M.: Temperature buffering in temperate forests: Comparing microclimate models based on ground measurements with active and passive remote sensing, Remote Sensing of Environment, 263, 112522, https://doi.org/10.1016/j.rse.2021.112522, 2021.
- Kemppinen, J., Niittynen, P., Riihimäki, H., and Luoto, M.: Modelling soil moisture in a high-latitude landscape using LiDAR and soil data. Earth Surface Processes and Landforms, 43, 1019–1031, https://doi.org/10.1002/esp.4301, 2018.
  - Kemppinen, J., Niittynen, P., Aalto, J., le Roux, P. C., and Luoto, M.: Water as a resource, stress and disturbance shaping tundra vegetation, Oikos, 128, 811–822, https://doi.org/10.1111/oik.05764, 2019.
- Kemppinen, J., Niittynen, P., Rissanen, T., Tyystjärvi, V., Aalto, J., and Luoto, M.: Soil Moisture Variations From Boreal Forests to the Tundra, Water Resources Research, 59, e2022WR032719, https://doi.org/10.1029/2022WR032719, 2023.
  - Kendall, M. G.: Rank correlation methods, 4th ed., Charles Griffin, London, 202 pp., 1975.
- Kolstela, J., Aakala, T., Maclean, I., Niittynen, P., Kemppinen, J., Luoto, M., Rissanen, T., Tyystjärvi, V., Gregow, H., Vapalahti, O., and Aalto, J.: Revealing fine-scale variability in boreal forest temperatures using a mechanistic microclimate model, Agricultural and Forest Meteorology, 350, 109995, https://doi.org/10.1016/j.agrformet.2024.109995, 2024.
  - Kopecký, M., Macek, M., and Wild, J.: Topographic Wetness Index calculation guidelines based on measured soil moisture and plant species composition, Science of The Total Environment, 757, 143785, https://doi.org/10.1016/j.scitotenv.2020.143785, 2021.
- 680 Krauss, L., Hauck, C., and Kottmeier, C.: Spatio-temporal soil moisture variability in Southwest Germany observed with a new monitoring network within the COPS domain, Meteorologische Zeitschrift, 523–537, https://doi.org/10.1127/0941-2948/2010/0486, 2010.
  - Lagergren, F. and Lindroth, A.: Transpiration response to soil moisture in pine and spruce trees in Sweden, Agricultural and Forest Meteorology, 112, 67–85, https://doi.org/10.1016/S0168-1923(02)00060-6, 2002.
- 685 Lantmäteriet: Orthophoto [dataset], https://www.lantmateriet.se/globalassets/geodata/geodataprodukter/flyg--och-satellitbilder/e pb ortofoto.pdf, last access: 20 August 2024, 2021.

- Lantmäteriet: Swedish Property Map, scale 1:10000 [map], https://www.lantmateriet.se/globalassets/geodata/geodataprodukter/topografi\_10\_nedladdning\_vektor.pdf, last access: 20 August 2024, 2023.
- 690 Larson, J., Lidberg, W., Ågren, A. M., and Laudon, H.: Predicting soil moisture conditions across a heterogeneous boreal catchment using terrain indices, Hydrology and Earth System Sciences, 26, 4837–4851, https://doi.org/10.5194/hess-26-4837-2022, 2022.
  - Larson, J., Wallerman, J., Peichl, M., and Laudon, H.: Soil moisture controls the partitioning of carbon stocks across a managed boreal forest landscape, Sci Rep, 13, 14909, https://doi.org/10.1038/s41598-023-42091-4, 2023.
- 695 Larson, J., Vigren, C., Wallerman, J., Ågren, A. M., Appiah Mensah, A., and Laudon, H.: Tree growth potential and its relationship with soil moisture conditions across a heterogeneous boreal forest landscape, Sci Rep, 14, 10611, https://doi.org/10.1038/s41598-024-61098-z, 2024.
- Laudon, H., Taberman, I., Ågren, A., Futter, M., Ottosson-Löfvenius, M., and Bishop, K.: The Krycklan Catchment Study—A flagship infrastructure for hydrology, biogeochemistry, and climate research in the boreal landscape, Water Resources Research, 49, 7154–7158, https://doi.org/10.1002/wrcr.20520, 2013.
  - Laudon, H., Hasselquist, E. M., Peichl, M., Lindgren, K., Sponseller, R., Lidman, F., Kuglerová, L., Hasselquist, N. J., Bishop, K., Nilsson, M. B., and Ågren, A. M.: Northern landscapes in transition: Evidence, approach and ways forward using the Krycklan Catchment Study, Hydrological Processes, 35, e14170, https://doi.org/10.1002/hyp.14170, 2021.
- Launiainen, S., Guan, M., Salmivaara, A., and Kieloaho, A.-J.: Modeling boreal forest evapotranspiration and water balance at stand and catchment scales: a spatial approach, Hydrology and Earth System Sciences, 23, 3457–3480, https://doi.org/10.5194/hess-23-3457-2019, 2019.
  - Li, R., Zhang, S., Li, F., Lin, X., Luo, M., Wang, S., Yang, L., and Zhao, X.: Impact of time-lagging and time-preceding environmental variables on top layer soil moisture in semiarid grasslands, Science of The Total Environment, 912, 169406, https://doi.org/10.1016/j.scitotenv.2023.169406, 2024.
- Liang, G., Stefanski, A., Eddy, W. C., Bermudez, R., Montgomery, R. A., Hobbie, S. E., Rich, R. L., and Reich, P. B.: Soil respiration response to decade-long warming modulated by soil moisture in a boreal forest, Nat. Geosci., 1–7, https://doi.org/10.1038/s41561-024-01512-3, 2024.
- Liang, W.-L., Li, S.-L., and Hung, F.-X.: Analysis of the contributions of topographic, soil, and vegetation features on the spatial distributions of surface soil moisture in a steep natural forested headwater catchment, Hydrological Processes, 31, 3796–3809, https://doi.org/10.1002/hyp.11290, 2017.
  - Lidberg, W., Nilsson, M., and Ågren, A.: Using machine learning to generate high-resolution wet area maps for planning forest management: A study in a boreal forest landscape, Ambio, 49, 475–486, https://doi.org/10.1007/s13280-019-01196-9, 2020.
- Mackay, D. S., Ewers, B. E., Cook, B. D., and Davis, K. J.: Environmental drivers of evapotranspiration in a shrub wetland and an upland forest in northern Wisconsin, Water Resources Research, 43, https://doi.org/10.1029/2006WR005149, 2007.
  - Mann, H. B.: Nonparametric tests against trend, Econometrica, 13, 245–259, https://doi.org/10.2307/1907187, 1945.

- McLaughlin, B. C., Ackerly, D. D., Klos, P. Z., Natali, J., Dawson, T. E., and Thompson, S. E.: Hydrologic refugia, plants, and climate change, Glob Chang Biol, 23, 2941–2961, https://doi.org/10.1111/gcb.13629, 2017.
- McMillan, H. K. and Srinivasan, M. S.: Characteristics and controls of variability in soil moisture and groundwater in a headwater catchment, Hydrology and Earth System Sciences, 19, 1767–1786, https://doi.org/10.5194/hess-19-1767-2015, 2015.
- Mei, X., Zhu, Q., Ma, L., Zhang, D., Liu, H., and Xue, M.: The spatial variability of soil water storage and its controlling factors during dry and wet periods on loess hillslopes, CATENA, 162, 333–344, https://doi.org/10.1016/j.catena.2017.10.029, 2018.
  - Meyer, H., Reudenbach, C., Wöllauer, S., and Nauss, T.: Importance of spatial predictor variable selection in machine learning applications Moving from data reproduction to spatial prediction, Ecological Modelling, 411, 108815, https://doi.org/10.1016/j.ecolmodel.2019.108815, 2019.
- Muñoz-Sabater, J.: ERA5-Land hourly data from 1950 to present, Copernicus Climate Change Service (C3S) Climate Data Store (CDS) [dataset], https://doi.org/10.24381/cds.e2161bac, last access: 3 December 2024, 2019.
  - Muñoz-Sabater, J., Dutra, E., Agustí-Panareda, A., Albergel, C., Arduini, G., Balsamo, G., Boussetta, S., Choulga, M., Harrigan, S., Hersbach, H., Martens, B., Miralles, D. G., Piles, M., Rodríguez-Fernández, N. J., Zsoter, E., Buontempo, C., and Thépaut, J.-N.: ERA5-Land: a state-of-the-art global reanalysis dataset for land applications, Earth System Science Data, 13, 4349–4383, https://doi.org/10.5194/essd-13-4349-2021, 2021.
- Murphy, P. N. C., Ogilvie, J., Meng, F.-R., White, B., Bhatti, J. S., and Arp, P. A.: Modelling and mapping topographic variations in forest soils at high resolution: A case study, Ecological Modelling, 222, 2314–2332, https://doi.org/10.1016/j.ecolmodel.2011.01.003, 2011.
  - Naturvårdsverket: The National Land Cover database: soil moisture index map, spatial resolution: 10×10 m, Swedish Environmental Protection Agency [map],
- https://geodatakatalogen.naturvardsverket.se/geonetwork/srv/swe/catalog.search#/metadata/cae71f45-b463-447f-804f-2847869b19b0, last access: 5 September 2024, 2022.
  - Nogovitcyn, A., Shakhmatov, R., Morozumi, T., Tei, S., Miyamoto, Y., Shin, N., Maximov, T. C., and Sugimoto, A.: Historical variation in the normalized difference vegetation index compared with soil moisture in a taiga forest ecosystem in northeastern Siberia, Biogeosciences, 20, 3185–3201, https://doi.org/10.5194/bg-20-3185-2023, 2023.
- Ochsner, T. E., Cosh, M. H., Cuenca, R. H., Dorigo, W. A., Draper, C. S., Hagimoto, Y., Kerr, Y. H., Larson, K. M., Njoku, E. G., Small, E. E., and Zreda, M.: State of the Art in Large-Scale Soil Moisture Monitoring, Soil Science Society of America Journal, 77, 1888–1919, https://doi.org/10.2136/sssaj2013.03.0093, 2013.
- de Oliveira, V. A., Rodrigues, A. F., Morais, M. A. V., Terra, M. de C. N. S., Guo, L., and de Mello, C. R.: Spatiotemporal modelling of soil moisture in an Atlantic forest through machine learning algorithms, European Journal of Soil Science, 72, 1969–1987, https://doi.org/10.1111/ejss.13123, 2021.
  - Pan, F.: Estimating Daily Surface Soil Moisture Using a Daily Diagnostic Soil Moisture Equation, Journal of Irrigation and Drainage Engineering, 138, 625–631, https://doi.org/10.1061/(ASCE)IR.1943-4774.0000450, 2012.
- Parajuli, K., Jones, S. B., Tarboton, D. G., Hipps, L. E., Zhao, L., Sadeghi, M., Rockhold, M. L., Torres-Rua, A., and Flerchinger, G. N.: Stone Content Influence on Land Surface Model Simulation of Soil Moisture and Evapotranspiration at Reynolds Creek Watershed, https://doi.org/10.1175/JHM-D-19-0075.1, 2020.

- Parent, A.-C., Anctil, F., and Parent, L.-É.: Characterization of temporal variability in near-surface soil moisture at scales from 1 h to 2 weeks, Journal of Hydrology, 325, 56–66, https://doi.org/10.1016/j.jhydrol.2005.09.027, 2006.
- Peichl, M., Nilsson, M., Smith, P., Marklund, P., De Simon, G., Löfvenius, P., Dignam, R., Holst, J., Mölder, M.,
  Andersson, T., Kozii, N., Larmanou, E., Linderson, M., and Ottosson-Löfvenius, M.: ETC L2 Meteo, Svartberget,
  2018-12-31–2023-12-31, ICOS RI [dataset], https://hdl.handle.net/11676/kF7lHD8qztNl\_5HdsSPWUmHs, last access:
  20 May 2024, 2024.
  - Petropoulos, G. P., Griffiths, H. M., Dorigo, W., Xaver, A., and Gruber, A.: Surface Soil Moisture Estimation: Significance, Controls, and Conventional Measurement Techniques, in: Remote Sensing of Energy Fluxes and Soil Moisture Content, CRC Press, 2013.
- Petropoulos, G. P., Ireland, G., and Barrett, B.: Surface soil moisture retrievals from remote sensing: Current status, products & future trends, Physics and Chemistry of the Earth, Parts A/B/C, 83–84, 36–56, https://doi.org/10.1016/j.pce.2015.02.009, 2015.
  - Piao, S., Yin, L., Wang, X., Ciais, P., Peng, S., Shen, Z., and Seneviratne, S. I.: Summer soil moisture regulated by precipitation frequency in China, Environ. Res. Lett., 4, 044012, https://doi.org/10.1088/1748-9326/4/4/044012, 2009.
- Potopová, V., Boroneant, C., Možný, M., and Soukup, J.: Driving role of snow cover on soil moisture and drought development during the growing season in the Czech Republic, International Journal of Climatology, 36, 3741–3758, https://doi.org/10.1002/joc.4588, 2016.
  - R Core Team: R: A Language and Environment for Statistical Computing, R Foundation for Statistical Computing, Vienna, Austria, 2023.
- Rasheed, M. W., Tang, J., Sarwar, A., Shah, S., Saddique, N., Khan, M. U., Imran Khan, M., Nawaz, S., Shamshiri, R. R., Aziz, M., and Sultan, M.: Soil Moisture Measuring Techniques and Factors Affecting the Moisture Dynamics: A Comprehensive Review, Sustainability, 14, 11538, https://doi.org/10.3390/su141811538, 2022.
- Riihimäki, H., Kemppinen, J., Kopecký, M., and Luoto, M.: Topographic Wetness Index as a Proxy for Soil Moisture: The Importance of Flow-Routing Algorithm and Grid Resolution, Water Resources Research, 57, e2021WR029871, https://doi.org/10.1029/2021WR029871, 2021.
  - Romano, N.: Soil moisture at local scale: Measurements and simulations, Journal of Hydrology, 516, 6–20, https://doi.org/10.1016/j.jhydrol.2014.01.026, 2014.
- Rosenbaum, U., Bogena, H. R., Herbst, M., Huisman, J. A., Peterson, T. J., Weuthen, A., Western, A. W., and Vereecken, H.: Seasonal and event dynamics of spatial soil moisture patterns at the small catchment scale, Water Resources Research, 48, https://doi.org/10.1029/2011WR011518, 2012.
  - Schönauer, M., Ågren, A. M., Katzensteiner, K., Hartsch, F., Arp, P., Drollinger, S., and Jaeger, D.: Soil moisture modeling with ERA5-Land retrievals, topographic indices, and in situ measurements and its use for predicting ruts, Hydrology and Earth System Sciences, 28, 2617–2633, https://doi.org/10.5194/hess-28-2617-2024, 2024.
- Sen, P. K.: Estimates of the Regression Coefficient Based on Kendall's Tau, Journal of the American Statistical Association, 63, 1379–1389, https://doi.org/10.1080/01621459.1968.10480934, 1968.

- Seneviratne, S. I., Corti, T., Davin, E. L., Hirschi, M., Jaeger, E. B., Lehner, I., Orlowsky, B., and Teuling, A. J.: Investigating soil moisture–climate interactions in a changing climate: A review, Earth-Science Reviews, 99, 125–161, https://doi.org/10.1016/j.earscirev.2010.02.004, 2010.
- SGU (Sveriges geologiska undersökning): Soil depth map, spatial resolution: 10×10 m [map], https://resource.sgu.se/dokument/produkter/jorddjupsmodell-beskrivning.pdf, last access: 20 August 2024a, 2024.
  - SGU (Sveriges geologiska undersökning): Soil types map, scale 1:25000 [map], https://resource.sgu.se/dokument/produkter/jordarter-25-100000-beskrivning.pdf, last access: 20 August 2024b, 2024.
  - Sikström, U. and Hökkä, H.: Interactions between soil water conditions and forest stands in boreal forests with implications for ditch network maintenance, Silva Fenn., 50, https://doi.org/10.14214/sf.1416, 2016.
- 805 Skogsstyrelsen: Utförda avverkningar (clearcuts carried out) [dataset], https://geodpags.skogsstyrelsen.se/geodataport/feeds/UtfordAvverk.xml, last access: 2 April 2025, 2024.
  - SLU (Sveriges lantbruksuniversitet): SLU Forest Map, spatial resolution: 25×25 m, Department of Forest Resource Management [map], https://www.slu.se/en/Collaborative-Centres-and-Projects/the-swedish-national-forest-inventory/foreststatistics/slu-forest-map/, last access: 7 April 2025, 2010.
- SLU (Sveriges lantbruksuniversitet): SLU Soil Moisture Map, spatial resolution: 2×2 m, Department of Forest Ecology and Management [map], https://www.slu.se/en/departments/forest-ecology-management/forskning/soil-moisture-maps/, last access: 8 April 2025, 2021.
  - Sørensen, R. and Seibert, J.: Effects of DEM resolution on the calculation of topographical indices: TWI and its components, Journal of Hydrology, 347, 79–89, https://doi.org/10.1016/j.jhydrol.2007.09.001, 2007.
- Stark, J. R. and Fridley, J. D.: Topographic Drivers of Soil Moisture Across a Large Sensor Network in the Southern Appalachian Mountains (USA), Water Resources Research, 59, e2022WR034315, https://doi.org/10.1029/2022WR034315, 2023.
- Svartberget Research Station: Meteorological data from Stortjärn, platform, 2016-07-02–2022-11-22, Swedish Infrastructure for Ecosystem Science (SITES) [dataset], https://meta.fieldsites.se/objects/SwldWWD0fJ6VII7VCCrGknQT, last access: 20 May 2024a, 2022.
  - Svartberget Research Station: Meteorological data from Svartberget, Åheden AWS, 2022, Swedish Infrastructure for Ecosystem Science (SITES) [dataset], https://hdl.handle.net/11676.1/v0bn\_ufBJ4vgq8Nen9d-Vqe5, last access: 20 May 2024b, 2022.
- Svartberget Research Station: Meteorological data from Svartberget, Hygget AWS, 2022, Swedish Infrastructure for Ecosystem Science (SITES) [dataset], https://hdl.handle.net/11676.1/ztFYjWV-ljPFra7V0z7NKHvg, last access: 20 May 2024c, 2022.
  - Takagi, K. and Lin, H. S.: Changing controls of soil moisture spatial organization in the Shale Hills Catchment, Geoderma, 173–174, 289–302, https://doi.org/10.1016/j.geoderma.2011.11.003, 2012.
- Teuling, A. J. and Troch, P. A.: Improved understanding of soil moisture variability dynamics, Geophysical Research Letters, 32, https://doi.org/10.1029/2004GL021935, 2005.

- Tyystjärvi, V., Kemppinen, J., Luoto, M., Aalto, T., Markkanen, T., Launiainen, S., Kieloaho, A.-J., and Aalto, J.: Modelling spatio-temporal soil moisture dynamics in mountain tundra, Hydrological Processes, 36, e14450, https://doi.org/10.1002/hyp.14450, 2022.
- USGS (U.S. Geological Survey): Landsat 8 Operational Land Imager (OLI) and Thermal Infrared Sensor (TIRS), Level 2 Science Product (Surface Reflectance), Path 194, Row 015, Collection 2, Tier 1, acquired on 2022-08-26 [dataset], https://earthexplorer.usgs.gov/, last access: 16 September 2024, 2022.
  - Van Sundert, K., Horemans, J. A., Stendahl, J., and Vicca, S.: The influence of soil properties and nutrients on conifer forest growth in Sweden, and the first steps in developing a nutrient availability metric, Biogeosciences, 15, 3475–3496, https://doi.org/10.5194/bg-15-3475-2018, 2018.
- Vereecken, H., Schnepf, A., Hopmans, J. w., Javaux, M., Or, D., Roose, T., Vanderborght, J., Young, M. h., Amelung, W., Aitkenhead, M., Allison, S. d., Assouline, S., Baveye, P., Berli, M., Brüggemann, N., Finke, P., Flury, M., Gaiser, T., Govers, G., Ghezzehei, T., Hallett, P., Hendricks Franssen, H. j., Heppell, J., Horn, R., Huisman, J. a., Jacques, D., Jonard, F., Kollet, S., Lafolie, F., Lamorski, K., Leitner, D., McBratney, A., Minasny, B., Montzka, C., Nowak, W., Pachepsky, Y., Padarian, J., Romano, N., Roth, K., Rothfuss, Y., Rowe, E. c., Schwen, A., Šimůnek, J., Tiktak, A., Van Dam, J., van der Zee, S. e. a. t. m., Vogel, H. j., Vrugt, J. a., Wöhling, T., and Young, I. m.: Modeling Soil Processes: Review, Key Challenges, and New Perspectives, Vadose Zone Journal, 15, vzj2015.09.0131, https://doi.org/10.2136/vzj2015.09.0131, 2016.
- Wang, F., Wang, G., Cui, J., Guo, L., Tang, X., Yang, R., and Huang, K.: Hillslope-scale variability of soil water potential over humid alpine forests: Unexpected high contribution of time-invariant component, Journal of Hydrology, 617, 129036, https://doi.org/10.1016/j.jhydrol.2022.129036, 2023.
  - Weiss, A. D.: Topographic position and landforms analysis, in: Topographic position and landforms analysis, ESRI Users Conference, San Diego, CA, 2001.
- Western, A. W., Grayson, R. B., Blöschl, G., Willgoose, G. R., and McMahon, T. A.: Observed spatial organization of soil moisture and its relation to terrain indices, Water Resources Research, 35, 797–810, https://doi.org/10.1029/1998WR900065, 1999.
  - Western, A. W., Zhou, S.-L., Grayson, R. B., McMahon, T. A., Blöschl, G., and Wilson, D. J.: Spatial correlation of soil moisture in small catchments and its relationship to dominant spatial hydrological processes, Journal of Hydrology, 286, 113–134, https://doi.org/10.1016/j.jhydrol.2003.09.014, 2004.
  - Wickham, H.: ggplot2: Elegant Graphics for Data Analysis, 2nd ed., Springer, New York, NY, 2016.
- Wild, J., Kopecký, M., Macek, M., Šanda, M., Jankovec, J., and Haase, T.: Climate at ecologically relevant scales: A new temperature and soil moisture logger for long-term microclimate measurement, Agricultural and Forest Meteorology, 268, 40–47, https://doi.org/10.1016/j.agrformet.2018.12.018, 2019.
- Williams, C. J., McNamara, J. P., and Chandler, D. G.: Controls on the temporal and spatial variability of soil moisture in a mountainous landscape: the signature of snow and complex terrain, Hydrology and Earth System Sciences, 13, 1325–1336, https://doi.org/10.5194/hess-13-1325-2009, 2009.
  - Winzeler, H. E., Owens, P. R., Read, Q. D., Libohova, Z., Ashworth, A., and Sauer, T.: Topographic Wetness Index as a Proxy for Soil Moisture in a Hillslope Catena: Flow Algorithms and Map Generalization, Land, 11, 2018, https://doi.org/10.3390/land1112018, 2022.

- Wu, D., Wang, T., Di, C., Wang, L., and Chen, X.: Investigation of controls on the regional soil moisture spatiotemporal patterns across different climate zones, Science of The Total Environment, 726, 138214, https://doi.org/10.1016/j.scitotenv.2020.138214, 2020.
  - Zhao, Y., Peth, S., Reszkowska, A., Gan, L., Krummelbein, J., Peng, X., and Horn, R.: Response of soil moisture and temperature to grazing intensity in a Leymus chinensis steppe, Inner Mongolia, Plant and Soil, 340, 89–89, 2011.
- Zhao, Z., Yang, Q., Ding, X., and Xing, Z.: Model Prediction of the Soil Moisture Regime and Soil Nutrient Regime Based on DEM-Derived Topo-Hydrologic Variables for Mapping Ecosites, Land, 10, 449, https://doi.org/10.3390/land10050449, 2021.
  - Zignol, F., Kjellström, E., Hylander, K., Ayalew, B., Zewdie, B., Rodríguez-Gijón, A., and Tack, A. J. M.: The understory microclimate in agroforestry now and in the future a case study of Arabica coffee in its native range, Agricultural and Forest Meteorology, 340, 109586, https://doi.org/10.1016/j.agrformet.2023.109586, 2023.
- Zignol, F., Lidberg, W., Greiser, C., Larson, J., Hoffrén, R., and Ågren, A. M.: Data repository: Controls on spatial and temporal variability of soil moisture across a heterogeneous boreal forest landscape, Mendeley Data, V1 [dataset], https://doi.org/10.17632/s8zg5ymkh6.1, last access: 13 April 2025, 2025.